

Naval Research Laboratory

Stennis Space Center, MS 39529-5004



UNCLASSIFIED

NRL/FR/7240--93-9422

Developing Automated Analysis Methods for Sea Ice Imagery: A Status Report with Recommendations

FLORENCE M. FETTERER

*Remote Sensing Applications Branch
Remote Sensing Division*

May 1993

Approved for public release; distribution is unlimited.

REPORT DOCUMENTATION PAGE			Form Approved OBM No. 0704-0188	
Public reporting burden for this collection of information is estimated to average 1 hour per response, including the time for reviewing instructions, searching existing data sources, gathering and maintaining the data needed, and completing and reviewing the collection of information. Send comments regarding this burden or any other aspect of this collection of information, including suggestions for reducing this burden, to Washington Headquarters Services, Directorate for Information Operations and Reports, 1215 Jefferson Davis Highway, Suite 1204, Arlington, VA 22202-4302, and to the Office of Management and Budget, Paperwork Reduction Project (0704-0188), Washington, DC 20503.				
1. AGENCY USE ONLY (Leave blank)	2. REPORT DATE May 1993	3. REPORT TYPE AND DATES COVERED Final		
4. TITLE AND SUBTITLE Developing Automated Analysis Methods for Sea Ice Imagery: A Status Report with Recommendations			5. FUNDING NUMBERS Job Order No. 5725126B3 Program Element No. 0602435N Project No. 3582 Task No. MOG Accession No. DN256010	
6. AUTHOR(S) Florence M. Fetterer			8. PERFORMING ORGANIZATION REPORT NUMBER NRL/FR/7240--93-9422	
7. PERFORMING ORGANIZATION NAME(S) AND ADDRESS(ES) Naval Research Laboratory Remote Sensing Division Stennis Space Center, MS 39529-5004			10. SPONSORING/MONITORING AGENCY REPORT NUMBER	
9. SPONSORING/MONITORING AGENCY NAME(S) AND ADDRESS(ES) Naval Research Laboratory Stennis Space Center, MS 39529-5004			11. SUPPLEMENTARY NOTES	
12a. DISTRIBUTION/AVAILABILITY STATEMENT Approved for public release; distribution is unlimited.			12b. DISTRIBUTION CODE	
13. ABSTRACT (Maximum 200 words) The 1990's will see a rapid increase in the amount of satellite data available for the analysis and forecasting of sea ice conditions. Planning is underway to bring altimetry from the Geosat Follow-on satellite, and synthetic aperture radar (SAR) imagery from the European Space Agency's Earth Remote Sensing Satellite (ERS-1), Canada's Radarsat, and Japan's Earth Resources Satellite (JERS-1) to the Navy/National Oceanic and Atmospheric Administration (NOAA) Joint Ice Center (JIC). In addition, JIC will continue to rely on visible and infrared imagery from the Advanced Very High Resolution Radiometer (AVHRR) sensor on the NOAA series of polar-orbiting satellites, and passive microwave data from the Special Sensor Microwave Imager (SSM/I) onboard the Defense Meteorological Satellite Program (DMSP) satellites. JIC has relied on manual analysis of AVHRR imagery in the past. The introduction of data from new sources will require automated methods for quickly and accurately analyzing data without necessitating additional personnel. This report surveys automated analysis methods which are being explored in the sea ice research community. Recommendations are made concerning automated analysis methods which are likely candidates for development under the Remote Sensing Applications Branch's 6.2 program, followed by transition to operational use at JIC. The long-term goal of 6.2 ice work is an automated system for near-real-time analysis and forecasting of ice conditions that uses all data available at JIC. Four milestones emerge as instrumental in meeting this goal, given the present status of automated analysis research, resources, and JIC requirements. <ul style="list-style-type: none"> • Develop methods for extracting ice parameters from merged data sets. • Create a prototype automated analysis system for Beaufort Sea SAR imagery. • Complete work on the Hough transform method for lead statistics from AVHRR imagery. • Develop methods of assimilating satellite-derived information into ice prediction models. These milestones can be met over the next 5 years if sufficient resources are available.				
14. SUBJECT TERMS remote sensing, artificial intelligence, data assimilation, satellite data			15. NUMBER OF PAGES 42	
			16. PRICE CODE	
17. SECURITY CLASSIFICATION OF REPORT Unclassified	18. SECURITY CLASSIFICATION OF THIS PAGE Unclassified	19. SECURITY CLASSIFICATION OF ABSTRACT Unclassified	20. LIMITATION OF ABSTRACT Same as report	

CONTENTS

I.	INTRODUCTION	1
II.	BACKGROUND	2
	A. The Navy/NOAA Joint Ice Center	2
	B. NRL Remote Sensing Applications Branch Resources	6
III.	ICE TYPE, CONCENTRATION, AND THICKNESS	8
	A. Current Status and Activities—SSM/I	8
	B. Recommendations—SSM/I	11
	C. Current Status and Activities—AVHRR	11
	D. Recommendations—AVHRR	16
	E. Current Status and Activities—SAR	16
	F. Recommendations—SAR	23
	G. Current Status and Activities—Altimetry	24
	H. Recommendations—Altimetry	28
IV.	LEADS AND RIDGES	28
V.	RECOMMENDATIONS — LEADS AND RIDGES	31
VI.	REMOTE SENSING DATA FOR IMPROVING ICE MODELS	31
VII.	RECOMMENDATIONS—MODEL INPUT FROM REMOTE SENSING	33
VIII.	CONCLUSIONS	33
IX.	ACKNOWLEDGMENTS	36
X.	REFERENCES	36

DEVELOPING AUTOMATED ANALYSIS METHODS FOR SEA ICE IMAGERY: A STATUS REPORT WITH RECOMMENDATIONS

I. INTRODUCTION

In the next decade the volume of satellite data available for ice analysis will multiply several times. Much of this increase will come from synthetic aperture radar (SAR) data. Automated analysis methods for extracting scientifically and operationally significant ice characteristics from this imagery are needed. Automated methods that take full advantage of multiple data sources, such as combined active and passive imagery, for improved ice analysis products are needed as well. This report suggests an approach for the Remote Sensing Applications Branch of the Naval Research Laboratory (NRL), which will meet these needs over the next few years.

Ice features that can be derived from satellite data are shown in Fig. 1. The satellite data emphasized in this report are from the Advanced Very High Resolution Radiometer (AVHRR), the Special Sensor Microwave Imager (SSM/I), satellite SARs, and satellite altimeters. These are chosen because data from these sensors are or will be available for operational use, and because the ice features shown by these data span the spectrum of ice characteristics needed for operational analysis. A brief survey of research on algorithms for sea ice data is given in the following pages. For the most part, these algorithms or automated analysis methods show promise for extracting

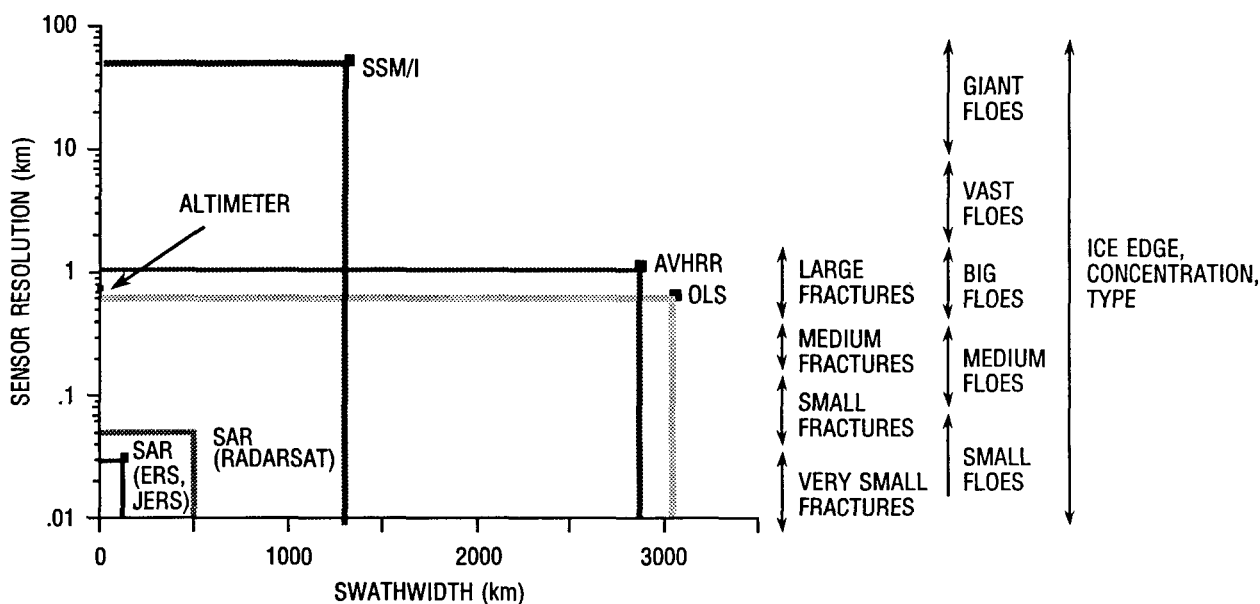


Fig. 1 — Satellite sensor swathwidth and resolution compared with World Meteorological Organization ice feature sizes. Ice edge position, concentration, and type is useful at any resolution. High-resolution information is important for specific operations, while greater swathwidth for near synoptic coverage is important for daily Arctic-wide analysis and climatologies. (after McNutt et al. 1988)

operationally important parameters, although they may have been intended for use in basic research. In an effort to be as current as possible, conference papers and workshop results are cited.

Recommendations are given throughout the text for specific areas of research which are likely to result in improved automated analysis capabilities. These recommendations take into account NRL resources and the plans of the Naval Polar Oceanography Center (NPOC) where operational sea ice analysis takes place. The long-term objective of the work suggested here is an automated system that efficiently makes use of all available data for near-real-time analysis and forecasting of ice conditions on a global scale. In the concluding section, four milestones are listed that are instrumental in making rapid progress toward this goal. A timetable for meeting those milestones is suggested.

II. BACKGROUND

A. The Navy/NOAA Joint Ice Center

While the power of automated analysis can be aptly applied to research problems concerning sea ice, the driving force behind the development of algorithms in the Remote Sensing Applications Branch is the increasing need for automated analysis methods at the Navy/NOAA Joint Ice Center (JIC). Techniques developed at NRL or elsewhere in the research community have a market at the JIC, and the Remote Sensing Applications Branch can insure the smooth transition of techniques from development to operational use.

The Navy side of the JIC is NPOC. NPOC's mission, and that of the JIC, is to analyze and to forecast global ice conditions in support of naval operations and government vessels. This mission is accomplished through the distribution of ice analysis products (see Table 1). The primary products of the JIC are the eastern and western Arctic analysis. Figure 2 shows an example of the western Arctic analysis. The "egg code" is used to show the concentration and type of ice in each outlined area. The primary data source for this product is AVHRR imagery. Although the JIC has a standing request with the National Oceanic and Atmospheric Administration's (NOAA) National Environmental Satellite and Data Information Service (NESDIS) for complete AVHRR coverage of the Arctic every day, the need for NESDIS to meet other data requests may mean that a given area outside NOAA's Gilmore Creek station mask in Fairbanks, AK, may be imaged as seldom as once a week. Dashed lines on the analysis in Fig. 2 indicate areas where boundaries are uncertain due to cloud cover or to lack of recent coverage. Clearly, the accuracy of this product will improve when microwave imagery, which is not affected by clouds, is regularly included in the analysis. Passive microwave imagery (such as that obtained from SSM/I brightness temperature data) can provide a check on ice edge position, while active microwave imagery (such as that obtained from SAR) can provide detailed information on concentration and type.

Table 2 shows the prospects for receiving satellite microwave data at JIC and at NRL. Because of its superior coverage, and the ease with which it can be analyzed and integrated into existing JIC products, SSM/I imagery may initially be the most useful data for JIC to include regularly in ice analyses. SAR, however, has far superior resolution and will approach synoptic coverage with the Earth Observing System (EOS) instrument. The EOS SAR will produce sea ice observations with a data rate several orders of magnitude greater than that of ERS-1. (Although the future of this particular instrument is uncertain, the trend is toward SARs with broader swaths.) SAR imagery presents the greatest challenge to automated analysis techniques, both because of the

Table 1 — Products of the Navy/NOAA Joint Ice Center

Product	Frequency
Western/Eastern Arctic Analysis	Once per week
Antarctic Analysis	Once per week
Alaska Region Analysis	Three times per week
Great Lakes Analysis	Three times per week
Western/Eastern Arctic 7-Day Forecast	Once per week
Western/Eastern Arctic 30-Day Forecast	Twice per month
Ross Sea 30-Day Forecast	Twice per month (seasonally)
Western/Eastern Arctic Seasonal Outlook	Once per year
Ross Sea/McMurdo Seasonal Outlook	Once per year
Special Ship Support	As requested
Navy-Only Products (Unclassified)	
Digital sea ice analysis file for PIPS model update	Once per week (through modem to FNOC)
NOAA-Only Products	
ADL Ice Edge	Once per week (through NMC TSO terminal)

volume of data which must be processed to analyze a given scene (which requires that algorithms be fast), and the sophistication that is necessary (simple image segmenters do not work well for a variety of reasons). The advent of SAR imagery at the JIC is perhaps the most compelling reason to increase our efforts toward automated ice analysis at NRL.

JIC products are created by visually interpreting hardcopies of AVHRR imagery and by manually compiling the results with other data sources. To produce analyses more efficiently, JIC hired a contractor to build the Digital Ice Forecasting and Analysis System (DIFAS). At a DIFAS workstation, the analyst can display digital AVHRR imagery from a data base of AVHRR passes, draw outlines of ice areas on the workstation screen, assign egg codes to areas, and print a final analysis product. DIFAS is now used to create the Alaska Regional Ice Analysis.

With DIFAS, JIC gained the ability to manipulate digital imagery. Rather than working with a hardcopy of a scene, analysts work with a digital image and apply enhancements to bring out ice features. However, DIFAS was not conceived as an image processing machine, and system capabilities are limited to contrast stretching, level slicing, and assigning color tables. In anticipation of future

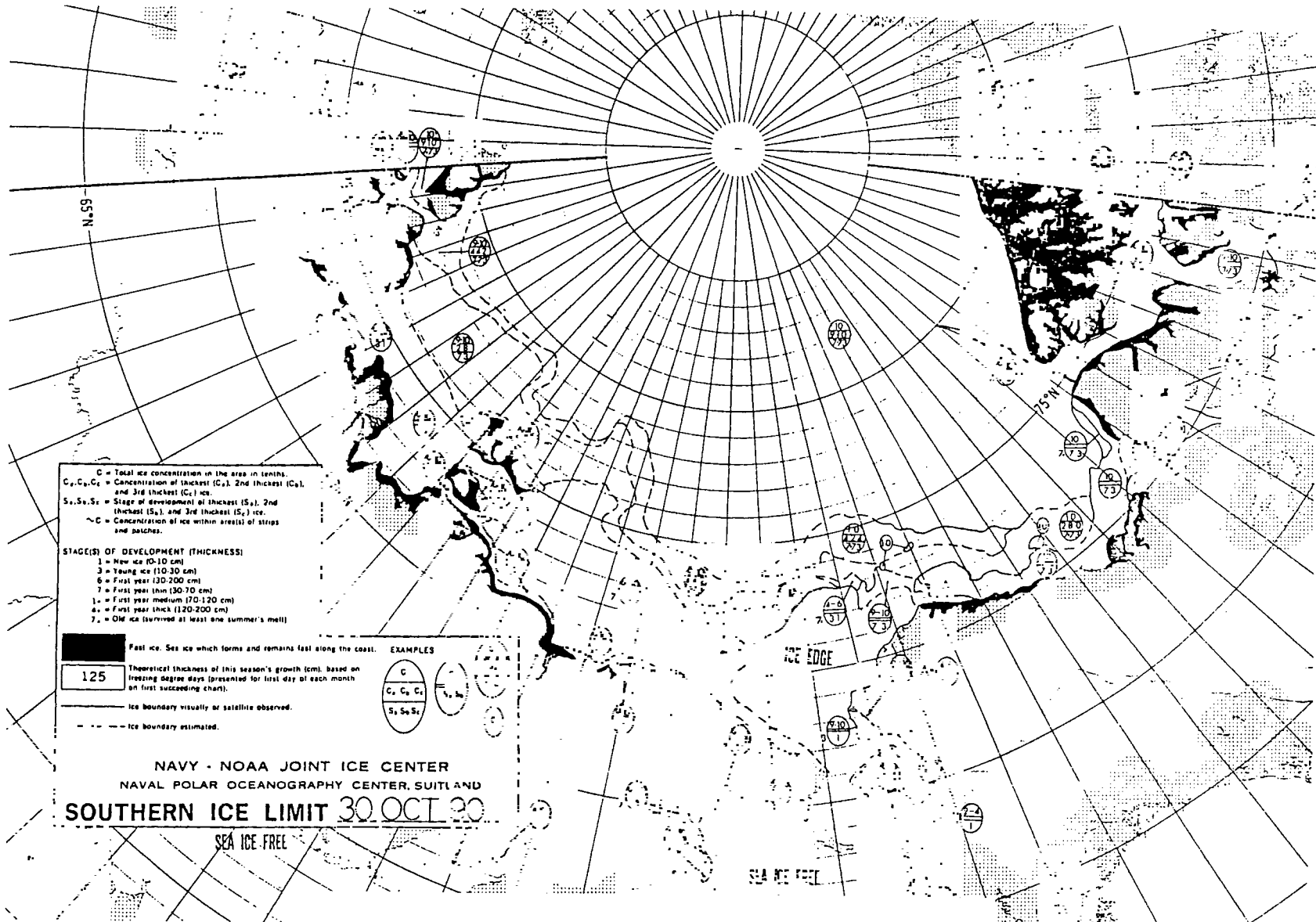


Fig. 2 — An example of the JIC western Arctic analysis.

Table 2 — Satellite Microwave Data at JIC and NRL

SAR	Resolution	Swathwidth	Time Line	Route to JIC	Route to NRL	Notes
ERS-1	30 m, 4 look 240 m, 32 look	100 km	Launch July '91 Duration 2-3 yr	SARCOM	SARCOM	98° inclination C-band VV pol 23° incidence angle
JERS-1	30 m, 4 look	75 km	Launch '92 Duration 2 yr	SARCOM	SARCOM	98° inclination L-band HH pol 35° incidence angle
Radarsat	30 or 100 m, nominally	50 or 500 km	Launch '95 Duration 5 yr	SARCOM	SARCOM	98° inclination C-band HH pol 20°-60° incidence angle Stereo imaging possible
Passive Microwave						
SSM/I	69×41 km (19 GHz) 60×36 km (22 GHz) 35×22 km (37 GHz) 16×10 km (85 GHz)	1300 km	Operational at present	Uncertain at this time, probably through distributed processing		
Altimeter						
ERS-1			Launch July '91	Uncertain at this time, probably waveform parameters include through distributed processing in fast delivery products		
GEOSAT (follow-on)			Launch '95	Uncertain at this time, probably no waveform data through distributed processing		
TOPEX			Launch '92			

needs, a DIFAS upgrade (DIFAS-Next) is now in the planning stages. However, the funding for DIFAS-Next is in doubt, and Tactical Environmental Support System (TESS) may take the place of DIFAS-Next. More importantly for NRL, either system will be UNIX based and will run X-Windows, which will allow for the easy transition of software from NRL to JIC.

JIC has begun to use satellite SAR imagery in an applications demonstration program during the first ERS-1 ice orbit. Imagery comes from the Alaska SAR Facility (ASF) in Fairbanks to JIC in near real time (6 h after satellite overpass) through a system of satellite links and landlines developed by NRL and NOAA. This data delivery system, called SARCOM, also includes hardware and software for compressing high-resolution (30 m) SAR imagery at ASF, and reconstructing it at JIC. ASF is operated by NASA and the University of Alaska. SAR data from ERS-1 and JERS-1 is received and processed at the facility. Eventually, data from Radarsat will be added to this set. The facility will also serve as a testbed for EOS SAR data handling. Each day ASF receives SAR imagery from a swath approximately 100 km wide and 2000 km long within the Fairbanks station mask. The European Space Agency (ESA) schedules SAR coverage. To obtain SAR data for its applications demonstration program, JIC has requested coverage of operationally important areas. The request has been made through the Programme for International Polar Oceans Research (PIPOR) group. PIPOR was formed to represent the needs of the polar data user community to ESA.

SAR products are operationally useful at JIC only if they are available soon after observation. For this reason, SARCOM was devised to transfer data quickly from ASF to JIC. Algorithms for ice motion (Kwok et al. 1990) and classification (Holt et al. 1989) similar to those developed for ASF by NASA's Jet Propulsion Lab (JPL) are used to analyze the imagery on a SAR workstation at JIC. The workstation, designed by JPL, consists of a Sun/470 with a Skybolt array processor, and assorted peripherals.

The SAR workstation at JIC creates products in near real time identical to those available from ASF (although JIC does not create a wave product). Products available from ASF are listed in Table 3. While NASA intends that the products be used for research, and for that reason released an "Announcement of Opportunity" for funding research programs, the announcement makes it clear that NASA is also interested in encouraging operational applications development.

With DIFAS-Next (or its equivalent) and the SAR workstation, JIC will have the computing power and digital imagery required for such advanced analysis techniques as data fusion. What JIC will not have, in all likelihood, is additional billets for people to operate the hardware systems or workstations. If the new system makes ice analysis easier and faster with algorithms from the research community, this may not be a problem. However, workstations could complicate the task and require a high level of expertise to use. The Remote Sensing Applications Branch is in a position to help prevent this from happening by ensuring that those algorithms being developed by the branch or its contractors are user friendly and accurate, and can be made an integral part of procedures for SAR analysis on the JIC SAR workstation or for AVHRR analysis on DIFAS or its successor. This will require flexibility in planning, since the prospect for JIC's access to additional satellite data, as well as the shape of DIFAS-Next, is evolving.

B. NRL Remote Sensing Applications Branch Resources

NRL will play a leading role in transitioning SAR algorithms from the research community to operational use at JIC. To facilitate this task, the Remote Sensing Applications Branch is developing

Table 3 — ERS-1 SAR Products from the Alaska SAR Facility

Image Products	Data Characteristics
Geo-coded Full Resolution	12.5-m pixel spacing 30-m resolution 80×100-km area
Geo-coded Low Resolution	100-m pixel spacing 240-m resolution 80×100-km area
Geophysical Products	
Ice Motion Vectors	Ice displacement vectors 5-km grid 100×100-km area (nominal)
Ice Type Classification	Ice type image 100-m pixel spacing 100×100-km area (nominal)
Ice Type Fraction	Fraction of each ice class 5-km grid 100×100-km area (nominal)
Wave Product	Wave direction and wavelength 6×6-km subsections From full-resolution image

the SAR Ice/Standard NRL Altimeter Processing System (SI/SNAPS, Fig. 3). The SNAPS side of the system will be used to process altimeter data from different satellites into Standard NRL Altimeter Record (SNAR) files. The standard format will allow all altimeter software to run with any altimeter data. The SAR side of the system replicates the SAR workstation, which resides at JIC. Ice motion and classification software, which runs at JIC and ASF, also runs on the SI system. In addition, SI has software for a SAR ridge and lead statistics algorithm developed by Vesecky and others at Stanford University (Vesecky et al. 1990).

NRL, in cooperation with NOAA and JIC, has prepared a planning document for ERS-1 SAR applications demonstrations programs. These programs will be carried out mainly at JIC. Figure 4 is a timeline from the applications demonstration plan. The timeline shows when hardware and software are expected to be in place at JIC and NRL, as well as a tentative schedule for applications demonstration programs. These programs are defined in the demonstration plan, but we anticipate that additional applications demonstration programs will be carried out at NRL and at JIC on an ad hoc basis as new algorithms developed at NRL and elsewhere in the research community mature. While the Remote Sensing Applications Branch is formally tasked with transitioning SAR algorithms, the branch can now, more easily than in the past, adopt a similar role for AVHRR and SSM/I algorithms as well. The growing commonality of software, hardware, and data between NRL and JIC facilitates this.

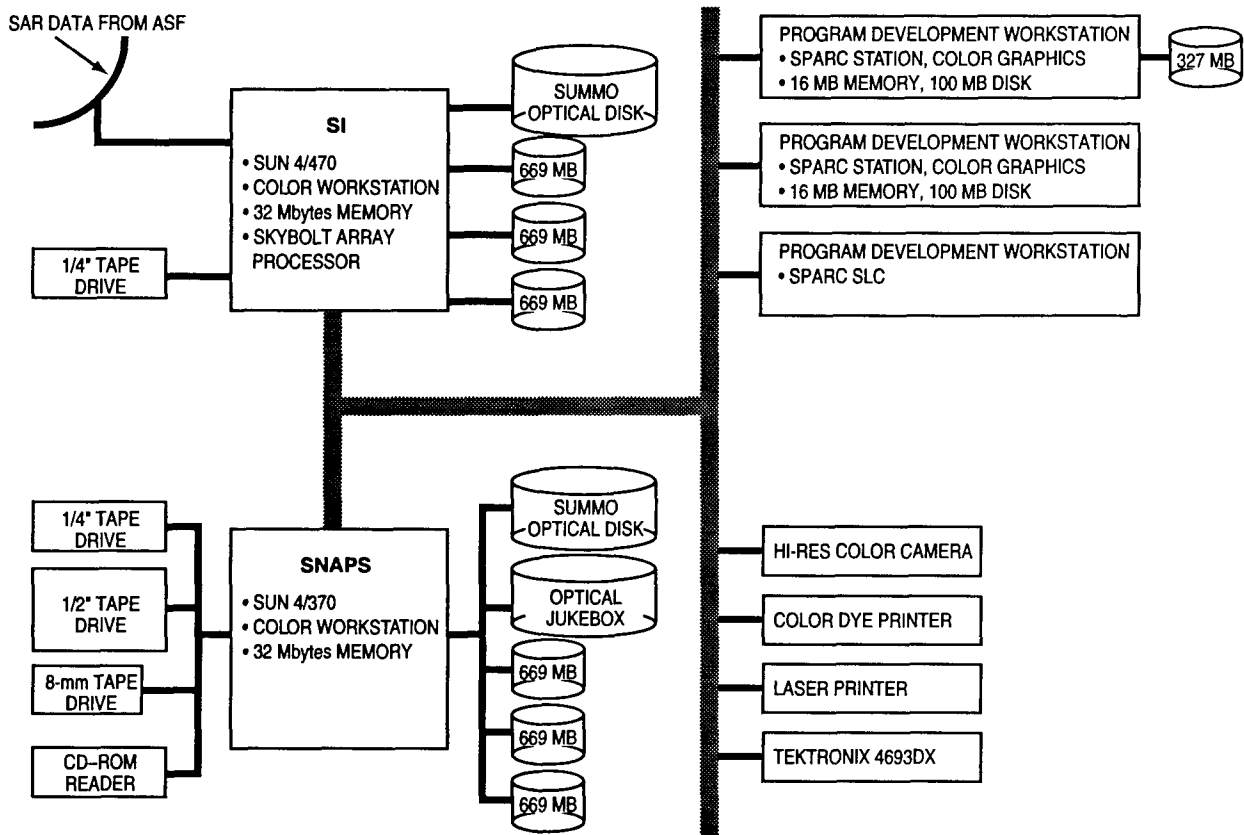


Fig. 3 — The SAR/Ice/Standard NRL Altimeter Processing System (SI/SNAPS)

III. ICE TYPE, CONCENTRATION, AND THICKNESS

Ice type and concentration are the ice parameters of primary importance to operational ice analysis, and are the parameters depicted on the JIC products through the egg code. Although ice thickness is perhaps the most important parameter from an operational standpoint, it can seldom be measured directly and must be inferred from ice type. These parameters are operationally important because they determine trafficability or the ease with which a vessel can move through or under the ice. They are of scientific interest for a number of reasons, not least of which is the role these parameters play in the global heat budget.

A. Current Status and Activities—SSM/I

Passive microwave brightness temperature data from the SSM/I sensor on board DMSP satellites can provide a nearly synoptic picture of ice-type composition and concentration on a 35- to 50-km grid. Four years of sea ice concentrations from the Nimbus-5 Electrically Scanning Microwave Radiometer (ESMR) demonstrated the utility of passive microwave images for compiling climatologies. Presently, SSM/I brightness temperatures are converted to a gridded ice concentration product at the Fleet Numerical Oceanography Center (FNOC) using a version of what has been termed the Atmospheric Environment Service (AES)-York University algorithm. (AES is the Canadian government office that operates the Ice Center Environment Canada (ICEC), an operational ice

center similar to JIC). JIC gets the product from FNOC over the Naval Environmental Display System (NEDS). Because the map projection used to display SSM/I data is different from the one JIC uses, the display is difficult to read and JIC finds the product cumbersome to use. This situation will be improved when SSM/I imagery can be warped to the JIC projection and displayed on DIFAS-Next or TESS. Brightness temperature data will probably reach National Meteorological Center (NMC) from FNOC through shared processing, and from there go to JIC, where an SSM/I algorithm can be run in-house. The importance of this capability to JIC is that refinements to the SSM/I algorithm, such as regional adjustments, can be easily implemented if the algorithm is being run in-house. In-house processing of brightness temperature data may begin in 1993, although no firm deadline has been set.

Several algorithms currently exist for SSM/I, and discussion concerning their relative merits is quite active. Algorithm development and validation efforts are ongoing at NASA/Goddard, University of Massachusetts, and York University. Only recently have results using the different algorithms been compared and then not rigorously in terms of Navy needs. Algorithm products show large differences in ice-type variability across the central Arctic. Differences in ice-type composition within a pixel can be great, especially in Antarctica, where there is little surface truth with which to tune the algorithms. The National Snow and Ice Data Center (NSIDC), which is archiving SSM/I data, has widely distributed brightness temperature data from SSM/I on a compact disk (CD-ROM). The accessibility to this information should generate increased interest in using the data and in validating the algorithms.

Algorithms for passive microwave instruments make use of the relationship

$$Tb = eT,$$

where Tb is the measured brightness temperature of the surface, e is the emissivity of the surface, and T is the surface's physical temperature. Different ice types and open water generally have different emissivities, which makes them separable in passive microwave data on the basis of brightness temperature. To derive the concentration of first-year ice, multiyear ice and open water within an SSM/I image pixel, it is necessary to use tiepoints. Tiepoints are the multichannel brightness temperatures of the three pure types on a triangular mixing diagram. Errors in concentration derived from the mixing diagram can occur when the emissivity of ice beneath the sensor is modified in some unanticipated way. For instance, snow cover can contribute to emissivity, and there is no way to parameterize this contribution (Carsey and Zwally 1986).

Due to the change in emissivity caused by liquid water on the ice, passive microwave estimates of ice type become unreliable with the onset of the melt season (Livingston et al. 1987). An additional source of error is the variability of emissivity from a given ice type. This variability arises from differences in ice history due to differences in climate and ice motion. Therefore, the variability is commonly regional in nature and could be accounted for through the use of regional tiepoints. Schweiger and Steffen (1989) have shown that an error of 10% in total ice concentration can be reduced to 3% in some places by using regional rather than global tiepoints. As part of the NASA-Team algorithm validation, ice concentrations derived from SSM/I, Landsat multispectral scanner (MSS), and AVHRR imagery were compared. Imagery was from the Beaufort, Bering, Weddell, and east Greenland Seas. To arrive at AVHRR ice concentration, a tiepoint algorithm for the visible channel was used. The algorithm assumes that pixels which are half ice and half water

have albedo halfway between that of ice or water alone. Such an algorithm is appropriate during periods of time when no new ice is forming. Ice concentration using the thermal AVHRR channels was much lower than that from Landsat; therefore, infrared concentrations were not used. The overall error of SSM/I compared to Landsat and AVHRR was 15%.

An interesting approach to improving ice-type concentrations derived from satellite passive microwave data was taken by Rothrock and Thomas (1988). The Kalman filter was used to blend surface temperature and advection information from drifting buoys with the microwave record to produce a smoothly varying record of ice concentration. The filter reconciles physical model predictions of ice-type concentration as it evolves in time with the temporal satellite data record to arrive at an optimal sequence of ice-type concentration. High-frequency variability in the observations can be given low weight and, therefore, will not produce an unrealistic (in a temporal sense) ice concentration record. The authors point out that the filter is a structure for rationally linking disparate data that relate to ice-type concentration, including other satellite data.

SSM/I data are now obtained by the Remote Sensing Applications Branch from FNOC or from the DMSP data stream. The data are used as inputs to the Polar Ice Prediction System (PIPS), comparison with ice concentration estimates from the Geosat altimeter, and data fusion studies.

B. Recommendations—SSM/I

Deriving ice type and concentration from SSM/I alone relies on automated algorithms that are in the process of refinement. There is no need for the development of automated data analysis methods by the Remote Sensing Applications Branch outside this effort. However, other ways in which to improve passive microwave algorithms involve using additional data sources. These will be treated in following sections.

The Remote Sensing Applications Branch should investigate methods of optimal assimilation and data blending (such as Kalman filtering), which may be useful data fusion, particularly for blending SAR with SSM/I.

C. Current Status and Activities—AVHRR

1. Enhancements to Aid Manual Interpretation

The operational status, synoptic view, and relatively fine resolution of AVHRR would seem to encourage the development of techniques for extracting ice type, concentration, and thickness using AVHRR imagery. A considerable amount of work in this area has been done by AES in Canada, where an Ice Status System for computer-assisted image analysis for observing and forecasting sea ice was developed in preparation for the near-real-time reception of AVHRR at ICEC. In one study, Condel et al. (1985) report encouraging results in classifying first-year sea ice and water into six classes using multidimensional maximum likelihood classification on imagery from the St. Lawrence region. Derived images used in the classification are a linear combination of channel 1 and channel 2 (which enhance albedo differences between ice types), a ratio of channels 1 and 2 (which enhance the difference between pack ice and clouds), a temperature map (created using the NOAA AVHRR processing algorithm (which corrects for atmospheric extinction), and a variance

map (where low values indicate spatial homogeneity and therefore areas of uniform ice type). The classification was compared with an operational ice chart, although quantitative results were not presented. Condel et al. (1985) note that before the method can be used operationally, more work is needed on the discrimination of clouds and ice and on sun and satellite viewing angle effects. Further, the analysis method will not work as well for multiyear ice, since the method depends on albedo, which changes with thickness only in saline, young ice. Because the reflective channels are used, it is a seasonal algorithm only.

Ramsey and Zerger (1986) derived a suite of image enhancement techniques to assist operational interpretation. For instance, they found that a linear contrast stretch worked well for reflective channels for general enhancement, while histogram equalization worked better for infrared channels. False color using contrast-stretched versions of channels 1, 2, and 4 loaded in red, green, and blue color guns improved ice/water contrast. Differencing channels 1 and 2 (channel 2 has a greater sensitivity to the ice/water boundary) and applying a gain and offset enhances the ice edge. A principal component enhancement was also found to be useful to the analyst. Ramsey and Zerger (1986) caution that their techniques have not been tested for different regions and seasons.

Generally, the emphasis in Canadian ice application research has been on assisted rather than automated analysis of AVHRR imagery. The prevailing belief is that at present, automated methods are too slow and cannot match the accuracy of an experienced human interpreter. This philosophy suggests that the analyst will be aided to the greatest degree by "canned" enhancements, especially when these are optimized for region or season. An example of this is the split-level enhancement developed by NOAA for the Bering Sea and Cook Inlet (Hufford 1981). Due to salinity differences, the temperature at which sea ice forms in the Bering Sea is different from that for Cook Inlet. The enhancement, which aids in locating the ice edge, maps pixels indicating near-freezing water temperature (different for the two regions) to black and ice temperatures to shades of gray (Fig. 5). As well as enhancing the ice edge, the method shows areas of near-freezing water that can be used to predict the formation and position of new ice when combined with meteorological data.

2. Surface Temperature Maps

Theoretically, ice thickness can be inferred from infrared measurements of bare-ice surface temperatures (Gloersen et al. 1974). Difficulties, which include the necessity of knowing air temperature at the surface and other variable weather conditions, as well as the structure of the ice cover (snow, for instance, can insulate ice) make it doubtful that the method will work with satellite data. However, accurate surface temperature maps in themselves are a worthwhile product. The SAR ice-type classification algorithm developed by the Jet Propulsion Laboratory (JPL) for ASF and JIC is meant to be used only where surface temperatures are below -5°C . Present plans are to use NMC temperature fields for temperature information. Because data for these fields are sparse, temperature information from AVHRR would be welcome and could improve the reliability of the JIC SAR classification product.

Ice surface temperatures can also improve the accuracy of the SSM/I ice classification product. Investigators at the Cooperative Institute for Research in Environmental Science (CIRES) in Boulder, CO, are studying the feasibility of arriving at an algorithm for deriving accurate sea ice temperatures in a way analogous to the method used for sea surface temperatures (that is, empirically, using buoy data), as well as by other means (J. Key, CIRES, personal communication 1990).

TEMPERATURE	GRAY SHADE	SURFACE TYPE
-4.5° to -4°C	White to Dark Gray	Clouds, Land
-3.5°C	Light Gray	Ice
-3.0°C	Dark Gray	Ice
-2.0°C	Medium Gray	Ice
-1.5°C	Black	Near-Freezing Water
-1.0° to 5.5°C	White to Black	Open Water

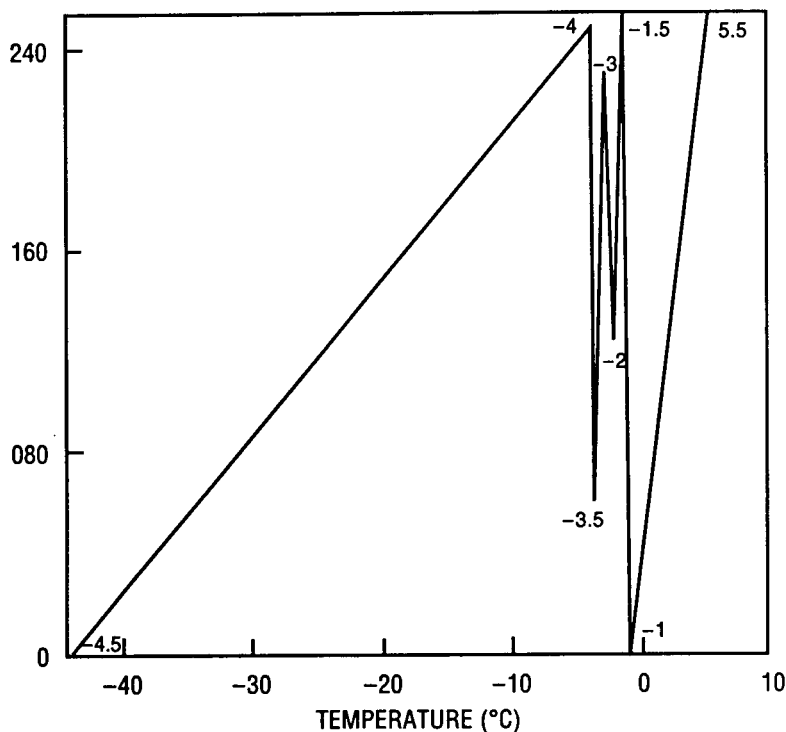


Fig. 5 — A split-level enhancement for infrared imagery to distinguish near-freezing water (from Hufford 1981)

3. Cloud Classification

To move beyond merely enhancing AVHRR imagery for a human analyst, a reliable method for automatically classifying cloud pixels must be found. This problem is difficult, since cloud pixels in infrared channels may be either warmer or colder than underlying ice in summer, as well as in winter. In the reflective channels, which are useless in the polar night, the albedo of clouds is similar to that of snow-covered surfaces.

The International Satellite Cloud Climatology Project (ISCCP), begun in 1983, has as its goal a global climatology of cloud radiance properties. An automated cloud detection algorithm for AVHRR was developed for the program, but because polar regions posed special problems, a

separate group was organized to test polar cloud algorithms (WMO 1987, cited in Key 1990). An example of an algorithm sparked by this study is one that uses the maximum likelihood decision rule to classify feature vectors composed of textural features from $2.5^\circ \times 2.5^\circ$ cells in the image (Ebert 1988). Eighteen surface and cloud categories were selected for training data. The algorithm correctly classified about 85% of the test cases. Such an approach would be useful to incorporate automated algorithms for AVHRR data if, instead of a pixel-by-pixel classification, it is acceptable to find cloud-contaminated cells. This approach is now taken manually as a precursor to using the Hough transform technique for lead orientation in AVHRR imagery (Fetterer et al. 1990). A compromise would then be made between a cell large enough for an adequate textural and spectral sample, yet small enough not to mask much of the image unnecessarily. Mixtures (cells which are partially cloudy) would be a problem, as would be the time required to choose training sets.

The need for a sophisticated cloud algorithm for polar regions has sparked one of the first uses of fused or merged data on the scale that will be possible in the 1990s. AVHRR imagery and passive microwave Scanning Multifrequency Microwave Radiometer (SMMR) imagery were merged to provide more information to a cloud-type algorithm on the surface beneath clouds (Maslanik 1989). The rationale behind the merged data set is that to interpret changing cloud properties, it is important to know what is happening beneath the clouds, since ice movement, changing ice concentration, and ice albedo all affect clouds. Using a summer Arctic image of merged AVHRR and SMMR data, a neural network classification of four surface and eight cloud types (such as low cloud over land or high cloud over ice) was compared with supervised maximum likelihood classification (Key et al. 1989). A back propagation neural network was used, with 7 input units (corresponding to five AVHRR channels and two SMMR channels), 10 hidden layer units, and 12 output units, which corresponded to the surface and cloud classes. Each seven-channel pixel in the merged image was used as input to the neural network for classification. The overall agreement between neural network classification and manual classification was 53%, with 1% of the image used for training the network. By comparison, supervised maximum likelihood classification (MLC) yielded 85% agreement, but 9% of the image was used for training (which would be impractical if many images were to be classified). Although the results with the neural network do not appear encouraging, the authors point out that one advantage of the method is that it handles large within-class variability (for example, the opacity of clouds in the low cloud over-ice class can vary widely), and a standard distribution of variability need not be assumed. Also, interpreting the weights in the hidden layer can point to the most important channels for correctly identifying a given class.

A neural network approach to classification may be well suited to automated classification of the multisource data upon which hopes for resolving ambiguities resulting from analysis of single source data are pinned. A neural network approach is nonparametric; that is, it does not rely on a priori knowledge of the statistical distribution of the data. Given the data sets likely to be merged for sea ice information, this is a distinct advantage. Benediktsson et al. (1990) compared neural network and statistical methods of classifying merged Landsat multispectral scanner (MSS) data (four channels), elevation data, and slope and aspect data from a Colorado forest. The objective was to classify forest tree types. The spectral response of the forest types is similar, so the additional data aid in distinguishing the types. The neural network method performed comparably with statistical methods. The authors note that for the best performance using statistical methods, weights must be assigned to the data sources. The assignment is done automatically in neural network classification. However, with neural network classification the best results are obtained with a truly representative training set, which may be difficult and time consuming to obtain from a given merged data set.

One drawback of neural networks is the time required to “train” a network. If a training set drawn from one merged data set can be used with all subsequent data sets, this is not prohibitive. However, using a neural network in this way may require that all image data be normalized in some way. Viewing angle effects must be removed from infrared and reflective channels, and SAR imagery must be calibrated.

Another algorithm that uses the merged SMMR and AVHRR data set described by Maslanik first identifies cloud-contaminated pixels using imagery over several days. The temperature and albedo of a pixel are compared with those on the day before and the day after. If the difference with either day exceeds a certain amount, which depends on the underlying surface given by SMMR, the pixel is classified as cloud (Key and Barry 1989). After cloud pixels are detected, cloud cover is classified using spectral and gray-level co-occurrence matrix (GLCM) textural features (Key 1990). The method differs from other similar methods in that texture values are assigned to each pixel (based on pixel neighborhood) rather than to a grid cell. Pixels classified automatically make a map of cloud classes. The classification agreement between pixels classified automatically and manually for a single image is 68.3% overall.

In summary, the cloud algorithms described here

- identified an area as containing a certain type of cloud over a certain surface type, often using MLC with textural and spectral features.
- identified cloud and surface types on a pixel-by-pixel basis using neural networks or MLC and spectral information from merged AVHRR and SMMR data. (This approach is slow for both methods of classification, and results are unacceptably inaccurate with neural networks, at least for the image studied.)
- relied on measuring temporal variability using a sequence of imagery.

None of these methods is ideal for masking cloud pixels in near real time on an image-by-image basis. A cloud-masking routine is desirable for enhancing imagery before manual interpretation or as a precursor to further analysis by automated means. In regions within the Gilmore Creek station mask, enough imagery is available to use time series variability (if the imagery can be processed quickly enough), but this would require acquiring and processing excessive amounts of imagery.

4. Trend Removal

AVHRR visible and infrared imagery usually contains gradients in temperature and albedo related to uneven illumination or regional variability in surface temperature. Often it is desirable to remove these gradients before processing imagery further. For example, the Hough algorithm for lead statistics from AVHRR (see Sec. IV on Leads and Ridges) requires a binary image of leads for input. Choosing a threshold to isolate leads from ice is often impossible unless gradients in illumination or temperature have been removed. Gradients should also be removed from imagery before the imagery is processed by a neural network or other spectral classifier. Eppler and Full (1991) developed a method of removing trends in imagery by fitting a third- or fourth-order polynomial surface to a gray-level image and then removing the surface, which models large-scale trends, from the image. Higher order surfaces degrade the result (if the objective is to segment the treated image into ice and water). There is some evidence that valleys in the higher order surfaces are related to lead distribution in images that contain leads.

D. Recommendations—AVHRR

AVHRR will be the mainstay of JIC ice analysis for years to come. Therefore, composing a library of canned enhancements (channel ratios, regional ice-edge enhancements, trend removal, and others) for use on the DIFAS system, with a notebook on using the enhancements, would be beneficial.

Pixel-by-pixel classification of clouds in AVHRR over ice-covered regions is a difficult problem that should not be attempted, since the payoff would be small. Cloudy areas can simply be removed manually before an AVHRR image is subjected to automated analysis (see Sec. IV). If the volume of imagery makes this impractical, an automated method of tagging cloud-contaminated blocks can be used, although the error rate is high. Successful cloud pixel identification waits for additional sensors and merged data.

One way to boost the value of AVHRR (and other infrared and visible band sensors) for ice analysis is to merge AVHRR with other data sources. Simply flickering collocated imagery from several sensors (SSM/I, AVHRR, SAR) boosts the analyst's interpretative ability. Merged data sets will be of even greater value if such sets can be used as input to ice classification algorithms that are of greater accuracy than algorithms that work on data from single sensors. Neural networks are one method of classification attractive for use with merged sets for the reasons given in Sec. C. Possible ways of becoming adept at using neural networks as image classifiers are to

- repeat the neural network method of Key with SSM/I and AVHRR, but with fewer classes for clouds—the purpose would be merely to detect cloud-contaminated pixels;
- attempt neural network classification of cloudy grid cells using a neural network for pattern analysis;
- attempt neural network classification using methods that do not rely on pixel spectral signatures, for instance, use shape and texture features.

Because of the potential value of surface temperature data as input to SAR and SSM/I classification algorithms, the Remote Sensing Applications Branch should remain apprised of ice temperature work as it develops, assist or collaborate if possible, and investigate the possibility of comparing AVHRR imagery archived at NRL with temperature data from the Arctic data buoy program or other sources.

E. Current Status and Activities—SAR

1. Ice Type Classification

SAR imagery of sea ice holds much promise for research and operational use because it combines high resolution with the ability to sense the surface through clouds. In general, older ice appears brighter in imagery than does younger ice, especially at shorter wavelengths (C-band, X-band). The salinity of first-year ice makes it more reflective than older ice, but because first-year ice is generally smooth, energy from the radar is reflected away from the antenna, and the ice appears smoothly dark in imagery. Radar energy penetrates farther into multiyear ice, which is less saline. The bright appearance of multiyear ice in imagery is due in large part to volume scattering from

empty brine pockets in the ice. For the most part, higher frequency SARs (C-band, X-band) are better for discriminating ice types, but lower frequency SARs (L-band) are better for detecting large-scale features, such as ridges and floe outlines.

Environmental factors can modify the expected signatures of first-year and multiyear ice. For instance, wet snow or meltwater can attenuate the signal in such a way that different types are no longer distinguishable. Open leads near the margin of the pack may fill with pancake ice as the leads freeze over. The pancakes are edged with shallow ridges caused by wave motion that grinds floes together. Pancake ice floating in a lead is highly reflective, and may cause a lead to be mistaken for a ridge in SAR imagery due to the bright, linear appearance of a lead filled with pancake ice (Carsey and Zwally 1986). Salt or frost flowers sometimes form on smooth ice as a result of vapor transport and can cause smooth young ice to appear as bright as multiyear ice in imagery. Although salt flowers are not a common occurrence, their presence can confound image segmentation based on brightness. Another difficulty is that both smooth water and new ice appear dark in SAR imagery, and it may be impossible to distinguish between transitional forms of young new ice (although this may not be important operationally). In short, when a human analyst looks at a SAR image, not only brightness but floe shape, knowledge of historical conditions in an area, and other factors are taken into account in deciding how ice in the image should be classified. This points out the desirability of an expert-system object-based approach for SAR analysis. For instance, if a segmented object in an image has a very high aspect ratio (like a lead) but is as bright as multiyear ice, the system might decide to place little weight on the high backscatter and to label the area "new ice."

An expert system for automated analysis, then, must be seen as the ultimate goal. However, for the analysis of some scenes, much simpler methods can give good results. Early work noted that tone or image brightness is not a unique classifier for ice type in SAR images (Lyden et al. 1984). This is in part due to the effect of speckle, or coherent noise in imagery. (Low-resolution SAR data from satellites is the result of many looks, or averaging; therefore, speckle is not a problem. Many papers on SAR algorithms treat methods of reducing speckle, as speckle can affect the performance of classifiers.) Also, the backscatter of an ice type can vary due to system effects. Because most airborne SARs must be considered uncalibrated radars, each image must be treated independently. Investigators have therefore been led to look toward classifiers that are nonparametric and unaffected by system effects. Texture measures are one example of such classifiers. Holmes et al. (1984), for instance, used GLCM texture measures to classify a SAR image with an overall accuracy of 65%. Later work by several investigators showed that texture measures for classification were not as successful as mean intensity and standard deviation of intensity; typically, the addition of texture did not improve results substantially (Skriver et al. 1986; Holback-Hanssen et al. 1989; Hirose et al. 1989; Garcia 1990).

Much Canadian work has been carried out under the aegis of the Canadian Radar Age/Type Algorithm Group (CRAGTAG), which has automated algorithms for ERS-1 and Radarsat imagery as its objective. A standard CRAGTAG image set consists of X-band airborne SAR imagery from Mould Bay in the Canadian archipelago and Seasat imagery from the Beaufort Sea. Using this imagery, Shokr (1990) evaluated the ability of first- and second-order texture parameters to classify five types of ice: multiyear, first-year-rough, first-year-smooth, young, and new (shown as MY, FYR, FYS, YI, and NI in the tables). He found multiyear ice easy to separate from the other types by using mean intensity or variance, but the mean intensity values for multiyear ice in Seasat imagery were twice that of the airborne imagery. The first-order texture parameters had variabilities

too large to make them useful as classifiers. Second-order parameters were derived from GLCM measures. Within limits, these measurements were found to be insensitive to the choice of window size and displacement vector. Multiyear ice was identified by a single value in both the Seasat and aircraft SAR images (Table 4). This surprising result points out the latitude one has in classifying imagery from different sensors when texture is used. The second-order measures used were inertia, uniformity, and entropy. Uniformity and entropy are highly correlated, and the variability of both increases with smoothness in the image. Therefore, the separability of smooth, young ice types is compromised. In general, texture or tone could be used to separate multiyear from younger ice, but neither could distinguish between the types of younger ice. Shokr (1990) noted that while GLCM measures are more universal classifiers than tone, the intense computation required may "defy operational requirements." However, Shokr suggested that an image with 255 gray levels was not necessary. The gray levels could be compressed to either 4 or 16 with similar results and reduced computation time.

Hirose et al. (1989) had similar results with the same data set. They note that redundant texture measures can be eliminated. Barber and LeDrew (1989) performed discriminate analysis using

Table 4 — Mean Values and Standard Deviations of Gray-Level and Texture Parameters for Ice Types from Mould Bay (MB) and Beaufort Sea (BB) Imagery (from Shokr 1990)

Ice Type	Image Data	Gray Level		Variance		Homogeneity		Contrast		Inertia	
		Mean	SD	Mean	SD	Mean	SD	Mean	SD	Mean	SD
MY	MB	57.38	11.56	22.52	2.811	0.0365	0.0253	245.98	140.881	0.1923	0.0863
MY	BB	120.30	30.63	48.726	7.678	0.0130	0.0136	1360.10	624.477	0.1908	0.0828
FYR	MB	28.53	7.84	11.144	2.111	0.0730	0.0379	62.29	49.45	0.0562	0.0271
FYS	MB	22.33	5.73	8.454	1.604	0.1099	0.0528	40.03	82.69	0.0280	0.0172
YI	BB	44.83	15.75	19.370	4.993	0.0348	0.0279	290.09	247.93	0.0445	0.0281
NI	BB	11.66	16.07	7.470	4.968	0.0861	0.0740	297.85	651.36	0.0205	0.0363

Ice Type	Image Data	Uniformity		Entropy		Entropy/Unifor.	
		Mean	SD	Mean	SD	Mean	SD
MY	MB	0.0307	0.0131	0.8101	0.0603	27.051	12.783
MY	BB	0.0290	0.0121	0.8261	0.0594	28.915	12.884
FYR	MB	0.0911	0.0437	0.6431	0.0903	7.911	4.846
FYS	MB	0.2061	0.1131	0.4866	0.1331	2.729	2.242
YI	BB	0.1308	0.0618	0.5880	0.0945	5.017	3.305
NI	BB	0.5038	0.3018	0.3051	0.2100	2.103	1.421

measures derived from the CRAGTAG Mould Bay data to reveal the most successful combination of five GLCM measures with different combinations of displacement vectors and orientations of those vectors. They found that discrimination is maximum when measures with different displacement vectors are used (but this involves substantially more computational effort). Five measures with different displacement vectors (10 measures in all) were successful in completely discriminating all four ice types in a test image. In a latter paper based on analysis of the same Mould Bay data set, Barber and LeDrew (1991) conclude that adaptive filtering to reduce speckle has a significant effect on texture, since it reduces local variance, but filtering does not significantly affect texture classification results on the images tested. In contrast to the work of Shokr (1990), Barber and LeDrew (1991) find that the choice of GLCM displacement vector length and orientation significantly affect classification accuracy. These conflicting results suggest that the usefulness of texture measures as nonparametric classifiers is somewhat belied by the sensitivity of results to such factors as GLCM window size.

A different approach to classification is used by Wackerman et al. (1988). Their fully automated algorithm makes use of the fact that although a histogram of image intensity for an entire image is typically unimodal and Rayleigh-like, a histogram for a local area commonly is bimodal, especially if the area contains enough pixels from each of two populations. Local tone information is therefore used to find ice-type boundaries. Histograms within a small window that moves across the image are computed. An ice class list with class statistics is kept. For each window position, the computed class (or classes, if the histogram is bimodal) is either merged with the current class or it becomes a new class. The number of classes in the image is arrived at automatically. The algorithm was tested with Marginal Ice Zone Experiment (MIZEX) data, but results are not shown. The Remote Sensing Applications Branch has received the code for this algorithm. Part of an East Greenland Sea MIZEX image has been run through the algorithm, but thorough evaluation has not been carried out. This algorithm shows a great deal of promise—if it can be made to run faster (it is extremely slow), if proper sensitivity parameters can be selected, and if class statistics for a given sensor's imagery can be tied unambiguously to ice type. However, because the algorithm is based on intensity statistics alone, it does not take into account contextual information. It may be a particularly good image segmentation method for use as a front end to an expert system.

2. The ASF/JPL Classification Algorithm

The classification algorithm that will be used at ASF is based on intensity and, ultimately, on a calibrated radar and a library of ice-type signatures, or a look-up table (Holt et al. 1989). The algorithm was tested using C-band imagery from the JPL airborne SAR. Imagery of the Beaufort Sea in March 1988 (and part of a data set used in SSM/I algorithm verification) was degraded to match expected ERS-1 imagery in resolution and noise level. The incidence angle of ERS-1 could not be matched for much of each image, but a correction was made to normalize images for changes in incidence angle across the swath. Coincident K-band Radiometric Mapping System (KRMS) data, as well as surface observations, were taken for comparison. Eight separate images were used.

The algorithm relies on the difference in backscatter between classes rather than on backscatter itself. A table of the ratio of mean backscatter values of first-year-rough, first-year-smooth, and new ice relative to multiyear ice was compiled using the eight images (Table 5). Classes are separated by about 4 dB. Mean multiyear backscatter varied from image to image by as much as 4.5 dB, but the backscatter ratios remained constant. This constant ratio allows the algorithm to work with an uncalibrated radar. First, a clustering algorithm uses a small fraction of image pixels

to find the number of classes, given expected separation between classes (4 dB). The cluster means are then compared to a look-up table. Eventually there will be separate look-up tables for region and season, but at present, the brightest cluster is assigned to multiyear ice. Then, each pixel in the image is assigned to a class using a minimum distance classifier. The class assignment is based on the mean value within a 3×3 pixel window around the pixel.

The algorithm performed well in a comparison with KRMS imagery. The disadvantage of the method is that it is sensitive to the width of the brightest cluster. The normal within-class variation of 0.5 dB results in 5% to 10% of multiyear pixels being misclassified. The error rises to 30% when variation is much greater than 5.0 dB. The cluster width depends in part on sensor calibration, and Holt et al. (1989) state that ERS-1 long-term calibration must be accurate to 2.5 dB. There is some debate over whether this calibration can be sustained. Future improvements will include the incorporation of wind and temperature data and possibly texture parameters. The algorithm is intended for use only during winter.

The Remote Sensing Applications Branch has evaluated the algorithm using ERS-1 data. Documentation of the algorithm's performance is in progress.

3. SAR for the Marginal Ice Zone

Because of its resolution, SAR imagery is particularly good for characterizing the marginal ice zone (MIZ). Wave propagation into ice can be seen in SAR imagery. The MIZ poses some special problems for automated analysis. The scale of features is quite variable. It may be more appropriate to classify areas with such types as "multiyear ice in consolidated first-year framework," as Holback-Hansen (1989) does with supervised maximum likelihood classification, rather than by typing ice on a pixel-by-pixel basis. Another approach to classification of complicated scenes in the MIZ and elsewhere is that of finding global texture and other measures for an image, and then sorting out the contributions from each ice type or ice matrix type using linear unmixing, following the method Holyer (1989) used with passive microwave imagery. One advantage of this method is that the image need not be segmented nor a window size chosen. The problem of the effect of varying scale is thus sidestepped. This method is not appropriate if a map of ice type is desired.

Table 5 — Normalized Backscatter Power Ratio of Four Different Ice Types Using C-Band VV Data at 25° Incidence Angle (from Holt et al. 1989)

	Normalized Backscatter Power Ratio DC 8 SAR (dB)	Standard Deviation of Ratios (dB)
MY	0	
FYR	-6.1	± .8
FYS	-11.6	± .9
NI/YI	-15.4	± .7

The ice edge can be compact or diffuse. If it is relatively diffuse, the idea of a “navigability index” based on floe size and percent open water makes sense. Banfield (1989) developed an algorithm for outlining floes to calculate floe size distribution. Burns et al. (1985) developed a computer-assisted technique for finding floe-size distribution based on chords through the image. The length of each chord within each floe is tallied manually, but the method could easily be adapted to work automatically with a segmentation algorithm, such as that described by Banfield.

The Programme for International Polar Oceans Research (PIPOR) proposes (1989) to use ERS-1 SAR from the Beaufort Sea to extract and find the size distribution of multiyear floes using digital techniques. ICEC will be doing this work to improve the accuracy of their ice analysis charts. PIPOR is a group founded to serve as an interface between the European Space Agency (ESA) and prospective users of ERS-1 SAR imagery.

4. Expert Systems for SAR Analysis

Shirtliff (1989) eloquently sets out the reasons for moving to expert systems for SAR analysis, given the large volume of data that will be produced by the upcoming generation of satellites:

The complex spatial and contextual information contained in SAR sea ice imagery requires an heuristic approach to analysis, more so than most other forms of image processing. A pixel-by-pixel approach to sea ice classification—the approach used in traditional digital image interpretation—ignores the syntactic (structural) and semantic (pragmatic) information that . . . is present in the SAR image. Syntactic reasoning would, for example, suggest that if several points in a region share similar backscatter properties and are part of a linear structure, that they are part of a pressure ridge. Semantic reasoning would suggest that if one is operating in a tactical time-frame, one need only process the data of regional interest, and seek to identify in order: open water, leads, thin/new ice, thin first-year ice, and seek to avoid regions of pressure ridging, glacial or old ice. The pixel based approach of traditional image processing is most inefficient at using these higher forms of knowledge representation and reasoning.

McAvoy and Krakowski (1989) have developed a prototype expert system for classifying SAR imagery based on information provided by the user. It can assist an inexperienced ice analyst or can be used as a training tool. The authors feel that their knowledge-based approach allows them to understand first what features are important before attempting fully automated classification. An interesting approach was taken to formulating rules based on the knowledge of several experts. Experts could not easily describe how they classify an image, and features that contribute to successful classification are not well documented. Therefore, a knowledge engineering tool was used to elicit construct names from six experts for features (such as angular floe, fine texture, ridging, and others) that aid in type classification. Thirty-one constructs made a preliminary knowledge base, which was augmented by regional ice climatology. Several types of rules were composed to identify ice types in four regions of the Canadian Arctic. The zones allow quick identification of ice type. Often only three user inputs regarding the ice being classified are needed. Accuracy is about 85% for old ice and 75% for other types.

A complete software package for interactive ice analysis, termed Iceman, has been developed to aid ice type and motion studies (Lee 1988). Iceman is fundamentally different from automated analysis routines and expert systems in that the system is merely an aid, or “toolbox,” for the

expression of an expert's knowledge. It does, however, incorporate automated analysis techniques in the form of texture-based ice classification (training areas are picked manually) and a correlation-based motion routine. The routine is meant to handle the fast and unpredictable motion in the MIZ, as well as that of the interior pack. General motion is determined through manual selection of a few tiepoints; these limit the search in the correlation routine, which fills in the motion grid. The concept is attractive for use in an operational environment, where the interactive classification routine could be applied to assist in manual interpretation of SAR imagery. Although the JIC SAR workstation will have fully automated routines for classification and motion, it is anticipated that higher resolution imagery and imagery for special projects will be analyzed manually, with the aid of drawing and annotation tools on the workstation. Tools for assisted analysis, such as a classifier similar to Lee's, can be incorporated into the JIC SAR workstation.

The problem of tracking ice in the MIZ is addressed in "Object Oriented Feature Tracking Algorithms for SAR Images of the MIZ" (Daida et al. 1990). The work is of interest to us here because of its object-based approach to image understanding. In this case, an unsupervised object-based method is used to select an appropriate ice motion algorithm for a given image pair. Automated methods for ice motion vary in their effectiveness, depending on how the ice is moving. For instance, an area correlation method works well in the central pack where motion is translational. In the MIZ, where floes may rotate, feature-tracking algorithms are called for. The method chooses an appropriate algorithm by first making an "abstraction" with each image. There are several levels of abstraction. The first is "class," of which there are two: ice and water. The second is "object." Objects are floes, which belong to the class of ice. The third level of abstraction is "properties," which belong to particular objects (floes), such as ice type, distinctive features, and ridging. Objects are depicted by a binary image of closed boundaries, and properties are depicted by various extracted features, such as gray tone, moment, and texture (Fig. 6). Objects and their properties are useful for matching features in two images because both boundary and interior information can be used, and the search space is somewhat limited. In this case, which algorithm to use is decided on the basis of how much area an object covers, although the method could include additional criteria.

A segmenter is used to arrive at the first level of image abstraction. The segmenter was chosen because it could generalize in the presence of noise while retaining sharp class boundaries. The segmenter does not require the number of classes to be input, and it is a nonparametric classifier. To arrive at the second level of abstraction, various methods of feature extraction are used. Feature extraction algorithms can be applied to an object, or a feature, such as a texture image, can be extracted using the entire image; the intersection of that feature image with the object can be used as that object's property.

The method of arriving at an image abstraction was tested using a 512×512 pixel Seasat image from the Beaufort Sea ice edge. After abstraction is complete, the tracking algorithm to use for particular objects is chosen based on rules; in this case the rule is of the form, "given an object with area X, use tracking algorithm A."

The segmentation and region growing methods appear to have some interesting characteristics that should be explored. The hierarchical method of assigning features to objects and objects to classes is a useful way of organizing image information. It also provides a structure for incorporating contextual information and for incorporating additional layers of information (i.e., additional data sources). Although these attributes were not used in the study, they may be invaluable for constructing a framework for an ice analysis system that can automatically sort and describe ice conditions or features as disparate as a large flaw lead off the Alaskan Coast and the complicated pattern formed

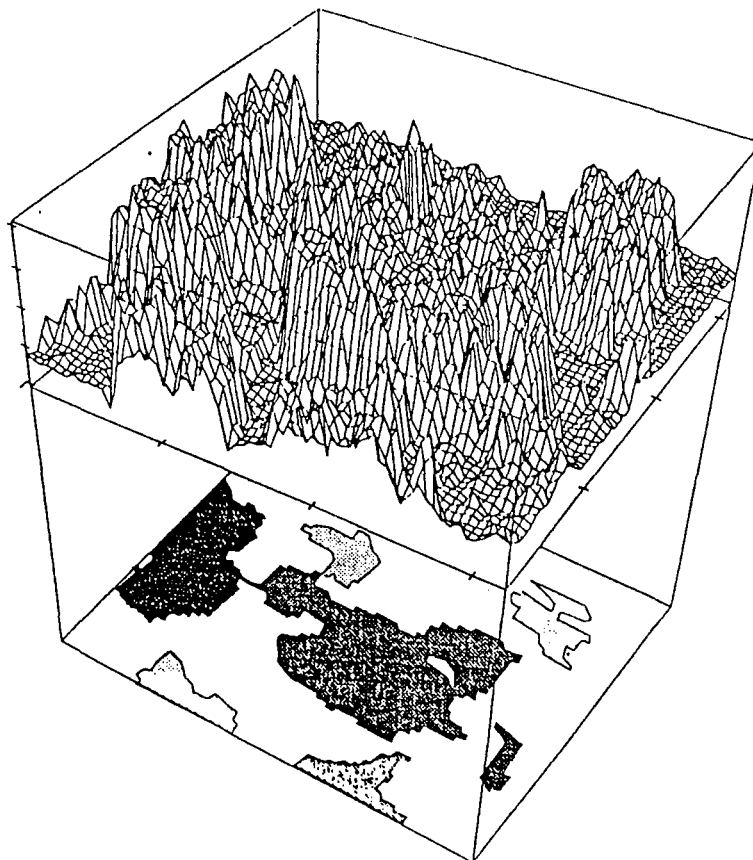


Fig. 6 — Object masking. An object plane (bottom) can serve as a window to image brightness data (top). (From Daida et al. 1990)

by floes of different size in the MIZ. While such a comprehensive system is far in the future, a prototype expert system that relies on object-based input can be constructed and can incorporate SAR feature extraction methods developed at NRL and elsewhere.

5. Summary

Three types of automated analysis methods are discussed here: (1) those that segment a SAR image on a pixel-by-pixel basis into ice classes on the basis of texture, backscatter, or both; (2) those that analyze an entire scene or scene section in one operation (such as the method of Holyer 1989); and (3) those which extract features (such as the floe outline method of Banfield and Raftery 1989). A fourth method, exemplified by Daida et al. (1990) unites other automated methods in an object-oriented, rule-based approach.

F. Recommendations—SAR

Rather than spend a great deal of time refining segmenters and feature extractors for SAR, work in the Remote Sensing Applications Branch should adopt the approach of Daida et al. and

construct an object-based expert system framework for the analysis of SAR imagery based on existing image operators. At this point feature extractors and segmenters have not been tested with enough images to prove their usefulness or universality. This lack of testing will change with the influx of imagery in the 1990s. A flexible object-based expert system will be able to accommodate increasingly sophisticated, more effective image analysis components. Several possible components for a prototype expert system already exist in-house. They include Wackerman segmentation algorithm and Holyer's method of scene ice-type composition through texture analysis. The second method has not been tested on SAR imagery but theoretically will work well with SAR. Suggestions for work toward the automated analysis of sea ice imagery are to

- compare Holyer's method with scene compositions arrived at by maximum likelihood classification or by Wackerman's algorithm. The method may be suitable in the MIZ, where pixel-by-pixel classification produces confusing results. The texture parameters from the analysis can be used as a field for object attributes in an expert system.

- test Wackerman's segmenter. The advantage of the segmenter is that it will segment any image. It does not depend upon a calibrated radar and a look-up table for backscatter, and the number of classes need not be specified. If other segmenters prove to be more effective at a later date they will be adopted, but resources should be concentrated on constructing the expert system rather than on optimizing a single (albeit important) component.

- construct a prototype expert system. The following could be the process:

- Choose a segmenter for deriving initial objects based on backscatter and tentatively label objects based on such attributes as brightness and aspect ratio. For instance, round objects are floes, dark objects with high aspect ratio are leads, etc.

- Add a texture feature plane. Each object would then have a texture attribute given by the area that the object covers on the texture plane.

- Map ridges for a ridge feature plane (leads should be identified as objects in the segmenter step, although wind-roughened water presents problems). Ridges and leads are discussed in the next section.

- Use rules to check consistency of ridge and texture attributes with initial labeling of objects. Refine the object map.

- Compute image statistics (ice-type concentration, lead and ridge statistics).

Regardless of the approach taken, such a system should ideally incorporate some way of judging when the object labeling is good enough to stop without adding new features. For instance, if backscatter adequately segments an image, there is no need to compute a texture plane.

G. Current Status and Activities—Altimetry

A satellite-borne altimeter is an attractive instrument for operational data because it operates at microwave frequencies (and is therefore unaffected by clouds), and its low data rate makes near-real-time processing possible. An altimeter cannot provide the synoptic coverage of an imaging radar. However, the Geosat data record provided a measurement every 0.7 km along track, and at

high latitudes orbit tracks become spatially dense. Altimeters are designed primarily for geodesy and mesoscale oceanography and function best over the open ocean where backscatter from the surface is easily modeled. A pulse emitted from the altimeter expands spherically and hits the ocean surface first at nadir. The "footprint" formed by the intersection of the pulse and the ocean surface is a circle that grows in diameter until the trailing edge of the pulse intersects the surface at nadir. The footprint then becomes an annulus of constant area and growing diameter as the pulse continues to expand. The echo of the pulse, recorded in a series of time gates, creates a waveform. The sharp slope of the leading edge of the waveform is a function of the sea surface height, and the gentle slope of the trailing edge is a function of the surface slope distribution, which can be related to windspeed.

Much of the ongoing work concerning altimetry and sea ice is reported in Hawkins (1990). Over sea ice, the power of the echo and the shape of its waveform are quite variable, but in general, the peak power is greater than that over water; however, the trailing edge of the waveform drops off sharply, giving the waveform a shape characteristic of specular reflection. No simple model can fully explain backscatter from sea ice, although Brown (1982) presented a model for reflection from first-year ice that explained the peaked, or "specular" component of ice waveforms as the result of coherent reflection from smooth facets of ice in the same horizontal plane. Ulander (1987) tested the model using Seasat waveforms with limited success but noted that to produce coherent reflection, ice facets must have a surface roughness of less than 0.25λ , or about 8 mm. Under most circumstances only nilas or calm water are this smooth.

The debate over the scattering mechanism at work when different ice types fall within the altimeter footprint is a continuing one. Although the mechanism is not completely understood, it is clear from empirical studies that operationally important ice parameters can be extracted from the altimeter data record. Dwyer and Goden (1980) developed an "ice index" for the GEOS-3 altimeter. This index uses a ratio of the average energy in a waveform to energy in the trailing edge of the waveform to mark the transition from water to ice. The ice index rises dramatically in value as the ice edge is crossed, reflecting a rise in peak backscatter power and a drop in power in the trailing edge. The GEOS-3 ice index was adapted for use with Geosat data. During a large part of Geosat's lifetime, the index was used to create an operational product for JIC that aided in fixing the ice edge in the presence of clouds (Hawkins and Lybanon 1989).

The Remote Sensing Applications Branch benefited from collaborative work with the Mullard Space Science Laboratory, University College, London. This collaboration led to improvements in the Geosat ice index and to a much wider comparison of AVHRR imagery with the Geosat altimeter parameters than had been carried out previously. Conclusions drawn from this comparison, as well as a thorough exploration of the possibilities for altimetry over sea ice, are reported in Laxon (1989). Also reported is a comparison of the extent of Antarctic sea ice from the Geosat altimeter with that from the SMMR. Agreement between the two sensors was excellent during the winter, but during the melt period the ice-covered area mapped through altimetry was greater than that mapped with SMMR. Laxon offers two possible explanations for this. The first is that meltwater is damping the wind waves seaward of the true ice edge, producing a return that could be mistaken for ice. The second, more likely explanation, is that the SMMR cannot detect the low concentration of ice near the edge due to melting, since the minimum concentration the sensor can reliably detect is 15%, and the problem worsens during the melt season. Therefore, the altimeter can be a more reliable indicator of ice edge than passive microwave, especially during melt season, and can fix the ice edge with greater precision in all seasons due to its higher (in the along-track direction) resolution.

Dwyer and Godin (1980) suggested that it may be possible to extract ice type from the altimeter record, since comparison with visible imagery suggested that the altimeter pulse echo was more powerful and waveforms more peaked in shape over younger, smoother ice. Ulander (1987, 1988) compared altimetry with SAR imagery and found that ice-type classes arrived at by manually interpreting the near-coincident SAR imagery were separable in most instances on the basis of backscatter value alone. While these results are encouraging, it is important to note that consistent results can be expected only over large expanses of relatively uniform ice. Robin et al. (1983) showed that if smooth areas cover only 0.01% of the surface near nadir, the shape of the waveform will be peaked with high backscatter, regardless of the nature of the remaining ice in the footprint.

Because altimeter returns are sensitive to the roughness of the surface near nadir, the waveform does not represent an "average" response from ice within the footprint. This limits its usefulness for unambiguous extraction of ice type or concentration, especially when ice is not homogeneous within the footprint. However, it may be possible to use the variability of altimeter parameters in combination with their values to demarcate zones of differing ice-type composition and floe size in areas where ice is not homogeneous on a scale comparable to the altimeter footprint.

Fetterer et al. (1988) compared Geosat altimetry with coincident SAR imagery over pack ice east of Greenland. The shapes of the altimeter waveforms were consistently peaked, and backscatter values were high over the MIZ (in the case studied, the MIZ appeared to be a band about 150 km wide filled with small, about 3-m-diameter floes). An abundance of smooth interstitial water can account for these returns. The transition from the MIZ to the pack itself, with its much larger floes, is marked by sudden increased variability in both the power and the shape of waveforms. Over the inhomogeneous surface, the altimeter does not transmit pulses and average echoes fast enough to sample the surface adequately, which results in instabilities in the on-board processing loops. The transition from pack to fast ice is marked by a sudden drop in pulse echo energy, stable pulse echoes, and a change in waveform shape from peaked to ocean-like. Presumably, this change occurs because within the fast ice, there are no areas of open water or new ice that might cause high-power, specular-type returns. The demarcation between MIZ, pack, and fast ice is probably not always as evident in the altimeter record.

Until altimeter backscatter from sea ice is better understood, a statistical or empirical approach to extracting ice parameters from altimetry must be used. Chase and Holyer (1988) used the method of linear unmixing to extract ice concentration and ice-type composition from waveform shape, with good results as measured by a comparison with coincident airborne passive microwave imagery. While it is generally agreed that waveform shape will depend on the smoothness of the ice surface and, by extension, ice type, extracting ice concentration from altimetry is much more problematic. McIntyre (1985) shows simulated waveforms from two areas with the same concentration of ice but different floe size distributions. The waveform shapes are quite different. Laxon (1989a) states that backscatter models show that unambiguous concentration measurements from altimetry may not be possible.

The altimeter has limited coverage and the interpretation of its data is uncertain. But because ice parameters influence backscatter measured by altimetry in a much different way than backscatter measured by an imaging radar, and because the altimeter is sensitive to parameters different from those that affect passive instruments, altimetry can best be used as an ancillary data source. For instance, the altimeter may be able to detect an oden (a vast expanse of ocean that suddenly freezes), even when the oden is not apparent in an infrared or visible image (J. Hawkins, NRL, personal communication 1990). Altimetry can be used to detect the ice edge, although more work

needs to be done to determine how the altimeter responds to diffuse or compact ice edges. The presence of swell within the ice edge can be detected in the altimeter record (Rapley 1984), and the effect of swell on an ice edge index must be considered. Figure 7 is a Seasat image of the Beaufort Sea ice edge. Clearly, it is not a simple image processing problem to find the ice edge in the image—the return from wind-roughened water is bright, and the floe size and the backscatter vary. Ice edge from altimetry would be a useful addition to the analysis of such an image.

The Mullard Space Science Laboratory has specified algorithms for two operational products from the ERS-1 altimeter over sea ice (Laxon 1989a). The first is the Quick Dissemination Sea Ice Margin, which is simply a list of the locations of the ice/ocean boundary. The list is intended for transmission to ships or offices where large data volume is a problem. The second, the Quick

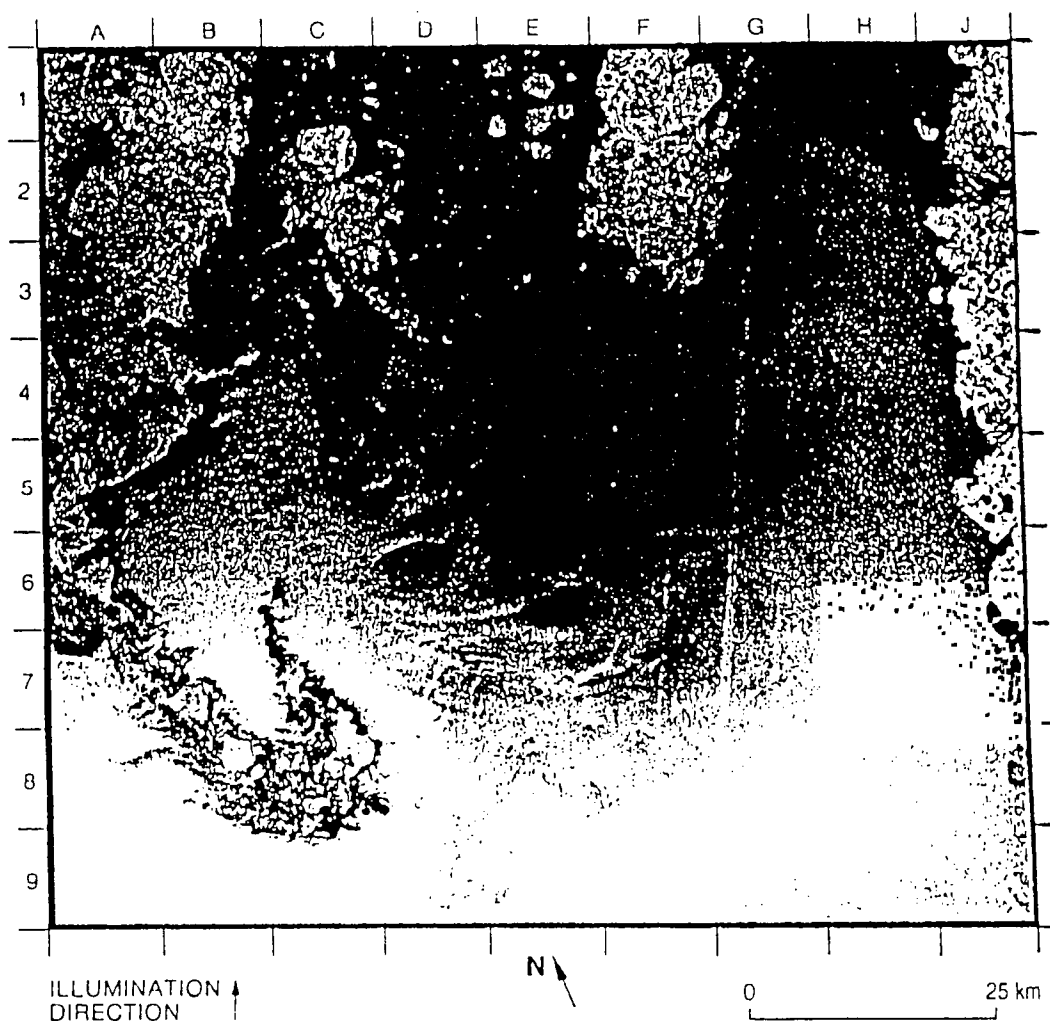


Fig. 7 — Seasat SAR image of ice and open water in the Beaufort Sea. The western portion of Banks Island is just visible on the upper right of the image. Wind-induced capillary waves cause patches of open water to appear bright. Individual floes of pack ice are identifiable by their rounded shape and distinct boundaries. (image from Fu and Holt 1982).

Dissemination Sea Ice Indices product, is a list of parameters derived from individual waveforms at a rate of 20 Hz. These parameters will be indicators of waveform power and shape.

Although ERS-1 has both a SAR and an altimeter, data from the SAR is offset from the altimeter track so that coincident altimetry and SAR imagery will not be possible. Near-coincident imagery is possible in polar regions where swaths for successive orbits overlap. But because power restrictions limit SAR data acquisition to 10% of each orbit, enough imagery for a comprehensive comparison of altimetry with SAR imagery over many regions and seasons may not be possible. Additional case studies from ERS-1 will further our understanding of altimeter response over sea ice.

At present, ERS-1 Quick Dissemination products are available to NRL and to JIC over the Shared Processing network. If possible, NRL should ensure that software for plotting the Quick Dissemination sea ice products is available at JIC for operational use and at NRL for data fusion and other studies.

H. RECOMMENDATIONS—ALTIMETRY

In preparation for the Geosat follow-on, prospective ice indexes based on Geophysical Data Record parameters should be investigated. For instance, the standard deviation of significant wave height can be used to mark the ice edge and may have advantages over the present ice index (Laxon 1989b). Laxon (1989a) also points out that a single ice index extracts limited information from altimeter data, since the effect of distinct physical properties of ice cannot be separated in the data record of a single ice index. For instance, the Geosat ice index depends on parameters automatic gain control (AGC) and voltage proportional to attitude (VATT), but VATT responds most strongly to changes in small-scale surface roughness, while AGC depends to a greater extent on both roughness and dielectric properties of ice. Therefore, ice index improvements should focus on finding the single most effective parameter or combination of parameters for demarcating the ice edge accurately. However, variability of parameters with ice conditions within the ice edge should be studied separately.

The ice edge given by SSM/I may have large errors, especially in summer. One way to examine those errors is to compare the ice edge given by some concentration contour in SSM/I imagery with that given by an altimeter ice index, after the manner of Laxon, but with the addition of AVHRR or SAR imagery. A concurrent investigation can be made into what conditions and at what concentrations the altimeter index indicates that the ice edge has been crossed. This will require a large set of nearly coincident SSM/I, SAR, AVHRR, and altimeter data.

Previous work (Fetterer et al. 1988; Laxon 1989a, b; Ulander 1988) showed that the fast ice edge often can be distinguished in altimetry. A "fast ice flag," which would mark the presence of fast ice and its sudden absence at spring breakup would be a useful additional information source for JIC. The Siberian or Alaskan coast is a likely site for a long-term comparison of AVHRR or ERS-1 Along Track Scanning Radiometer imagery with altimetry, as these coasts have wide fast ice shelves, and are largely within the Gilmore Creek station mask for ERS-1 and NOAA polar orbiters.

IV. LEADS AND RIDGES

It is important, both operationally and scientifically, to develop our ability to detect and map leads and ridges using satellite data. A heavily ridged area can be difficult or impossible for an ice breaker to traverse. Ridges usually coincide with under-ice keels, which are a hazard to submarines.

Ridges serve as identifying features to help distinguish first-year ice from young ice in SAR imagery. Leads are an extremely important conduit for heat flux in polar regions. From an operational standpoint, submarines can easily surface through large leads, and a change in the number of leads can indicate that the pack is undergoing compression, which affects trafficability.

Areas of ice cover that have undergone intense deformation have an elevated brightness temperature in passive microwave data, which leads to inaccurate estimates of the multiyear ice concentration (Eppler 1989; Cavalieri et al. 1991). It is important, therefore, to be able to map such areas or to understand their regional distribution to gauge the accuracy of SSM/I ice-type estimates. Heavily ridged ice is evidence of deformation.

For leads and ridges, as with the ice parameters discussed in previous sections, what is ultimately needed is both a climatology of statistics and an analysis suitable for tactical decision making and near-real-time distribution. High-resolution satellite imagery is needed to address both needs. Although the distribution of lead widths is not well known throughout the Arctic, it is believed to follow a power-law relationship. The frequency of occurrence falls rapidly with width (Wadhams et al. 1985), although the exact form of this relationship is probably site specific. Therefore, lead analysis using AVHRR infrared or visible imagery will neglect many small leads. If one is interested only in leads on the order of 1 km wide, this drawback is not serious. The difficulty with using AVHRR for lead statistics will be mitigated somewhat when the radiative transfer function, which describes the signature of leads in AVHRR infrared imagery, is modeled (efforts in this direction are underway at CIRES) and if a relationship between large lead size and orientation and that of small leads can be found. For instance, it has been suggested in a number of places that lead patterns may exhibit fractal properties. The ability to merge low-resolution AVHRR easily with high-resolution SAR on the SI/SNAPS system at NRL will aid in investigations of this type.

Few satellite sensors other than SAR have resolution high enough to image ridges. Askne and Johansson (1988) constructed a model of SAR backscatter from ridges that allowed them to draw several general conclusions. For instance, ridges should be more easily distinguishable in C-band than X-band imagery, because the background ice will appear more uniform at longer wavelengths. Along-track and cross-track ridges will appear different. And because the ice in ridges is anisotropic as compared to the surrounding ice, ridges should show up well in cross-polarized mode imagery.

In satellite SAR imagery, ridges are assumed to appear as an interlacing network of bright filaments, while leads appear as dark, somewhat linear features. (There is no conclusive proof that all bright, linear features in SAR imagery are ridges.) Vesecky et al. (1990) derived an automated method for estimating lead and ridge density, the distribution of lead area and orientation, and the distribution of ridge length and orientation using SAR imagery. To extract ridge features, a threshold is applied to an image to isolate bright features, and a simple line detector is used to find line filaments. Pixels that belong to both a bright feature and a line filament are counted as ridges. The resulting ridge features are thinned to a width of one pixel, so feature intersections and end points are more easily determined. A "ridge" is defined as a segment between nodes, and ridge length and orientation statistics are computed according to this definition. Orientation is that of a least-squares fitted line between nodes. Lead statistics are extracted by a similar but simpler method.

The Vesecky et al. algorithm for lead and ridge statistics will be installed on the JIC SAR workstation and on the Remote Sensing Applications Branch SAR workstation. Because we are charged with testing and evaluating this algorithm for JIC, it is necessary to look at the method

critically. The algorithm was tested using only one image, a Seasat image of the Beaufort Sea (although further testing is underway). It will be important to secure ground truth for the algorithm at the first opportunity. The method used to choose a threshold for ridges (take the brightest 20% of pixels) and for leads (examine the image histogram and choose the junction between dark plateau and bright peak) cannot be expected to work well in all images. Leads that appear bright because of a wind-roughened surface or salt flowers pose a problem. The limitations of the algorithm must be defined better before it is ready for operational use at JIC.

While ridges cannot be mapped in AVHRR imagery, large leads appear as warm linear features in infrared imagery and as dark features in visible imagery. Fetterer and Holyer (1989) developed a method for automatically extracting lead orientation using the Hough transform to find lines (or lead segments) in AVHRR infrared or visible imagery. To work effectively, a binary image of leads must be created, but this has not been done automatically. Improvements were made to the method so that not only orientation but lead or lead segment size is extracted automatically through the transform (V. Cambridge, Sverdrup Technology, personal communication). Computer functions were written to run the algorithm and to display the results as rose diagrams of lead direction and size overlaid on an image. The method was used to analyze AVHRR imagery north of Greenland in support of the ICESHELF acoustic exercise (Fetterer et al. 1990).

The Hough transform method for lead statistics, in its present form, takes a raster-based image of leads and represents those leads as objects in Hough transform accumulator space. The location of each lead pixel is known, as is the orientation of the lead segment of which it is a member. Such an object-based representation makes it easy to apply rules for the definition of leads and lead complexes and to extract statistics based on those (changeable) definitions. Key et al. (1990) used an object-based approach for extracting lead statistics from a Landsat MSS image. A dynamic threshold was used to create a binary image of leads, in which lead fragments are located with a region-growing procedure. The orientation, width, and length of these lead objects was calculated. Rules were used to merge objects that are close and have similar orientations and to discard small objects. One advantage of the rule-based approach, the authors note, is that it gives the flexibility needed to decide upon a definition of "lead," since leads are often linear at very large (100 km) and small (10 km) scales, but curved and disjointed at medium scales (30 to 60 km).

The distribution and geometry of leads and ridges has not been well described or linked to atmospheric and oceanographic forcing in a rigorous way on a large scale. Understanding how and when lead complexes form in ice and the processes that occur over the lifetime of a single lead are objectives of the Arctic Leads Accelerated Research Initiative (Leads ARI), sponsored by the Office of Naval Research. NRL has been funded to compile and process 3 years' worth of Arctic-wide AVHRR imagery. This imagery will be used by investigators studying the characteristics and distribution of leads. A 3-year climatology of lead statistics can be compiled using this data set and the Hough transform method. The climatology will be similar in form to a contractor-created method for JIC, using DMSP OLS imagery from which leads were traced by hand.

Satellite altimetry should not be overlooked as a source of information about leads. The signature of a wide, wind-roughened lead will be the same as that of open water. When a lead filled with smooth water or new ice is near nadir, the altimeter waveform will be characteristic of specular reflection. Laxon (1989a) suggests that the sensitivity of the altimeter to the presence of leads or smooth open water can be used to distinguish between areas of complete ice cover and areas with

some open water within the pack. This information may be useful in assessing areas subject to error in passive microwave derived concentrations (which may not be accurate where ice is present in high concentrations).

V. RECOMMENDATIONS — LEADS AND RIDGES

The comprehensive AVHRR data set processed by the Remote Sensing Applications Branch for the Arctic Leads ARI should be used to leverage other ice research efforts. A comparison between lead statistics from SAR and those from AVHRR can be made, and a better understanding of how the AVHRR images leads of different sizes will be gained. This, in turn, will enhance confidence in statistics drawn from AVHRR using the Hough transform or other methods. The Lead ARI will include a field experiment during which surface truth for SAR, AVHRR, and passive microwave sensors will be collected. This experiment may provide some of the ground truth needed to validate the Vesecky et al. algorithm for ridges as well.

The Hough transform method for lead statistics is ready for transition to a 6.3 program and operational use. Rather than transition the method in its present form, additional 6.2 level work is recommended to automate threshold selection for the creation of a binary image. Also, a prototype rule-based system, which builds on the Hough transform method, should be attempted.

A comparison between SAR imagery and SSM/I can be carried out using SAR imagery archived at NRL during the ERS-1 lifetime. A merged SAR and SSM/I data set would prove invaluable in learning seasonal and regional limitations and advantages of both SAR and SSM/I for ice analysis. Two methods of improving SSM/I ice-type retrievals could be investigated with this data set. The first would be to use SAR imagery to identify where SSM/I multiyear ice concentrations might be erroneous due to deformation, perhaps by using ridge density from the Vesecky algorithm as a measure of deformation. The second would be to use multiyear, first-year and open water concentrations from SAR to fix tiepoints for the SSM/I algorithm. The creation of a merged data set will require investigation into what time separation between images to be merged is tolerable. It is also important to learn whether or not information derived from SAR imagery can be extrapolated beyond the SAR swath. A similar study is proposed under PIPOR for the Weddell Sea (PIPOR Research Plan 1989).

VI. REMOTE SENSING DATA FOR IMPROVING ICE MODELS

Numerical ice models are important for operational ice nowcasting and forecasting. These models provide the only method whereby spatial coverage can be made complete (by interpolation) and forecasts can be made (by time-stepped evolution) for output fields of ice characteristics, such as concentration and motion. In addition, thickness, which cannot be remotely sensed, can be modeled.

Ice forecast models are of three kinds: drift models, which merely predict ice motion; coupled dynamic/thermodynamic models, which take changing ice thickness into account; and coupled ice/ocean models. The last of these models is being developed but has not been used operationally (Joint Oceanographic Institutions, Inc. 1987). Empirical drift models predict the movement of the ice in response to wind based on buoy data. Drift models are usually adequate for short-term forecasting (less than about 5 days). For long-term forecasting, however, the effect of heat transfer on ice growth and melting must be included.

Operational models are usually derived by modifying research models. This has been the case for the drift models used at ICEC (McNutt et al. 1988), and it is the case for the PIPS used by JIC. PIPS evolved from the Hibler dynamic/thermodynamic model (Hibler 1979). The description of PIPS given here is taken from Preller and Posey (1989). Unlike the earlier drift model used by JIC, PIPS takes into account internal ice stress by modeling changes in ice concentration, thickness, and ice deformation. Deformation can redistribute thin ice into thick ice. Through the means of deformation, the model incorporates the effect of ridging. The inclusion of thermodynamic interaction as well makes PIPS a dynamic/thermodynamic model.

Atmospheric forcing for PIPS is provided by the Navy Operational Global Atmospheric Prediction System (NOGAPS). In addition to surface pressure fields from which geostrophic winds are derived, NOGAPS supplies some of the terms needed to compute air stress and thermodynamic interaction, such as vapor pressure, air temperature, incoming solar radiation, and surface heat flux. Oceanic forcing is provided in the form of monthly mean ocean currents and heat fluxes by a separate coupled ice/ocean model. PIPS can be initialized through using the previous day's 24-h forecast file of ice thickness, concentration, drift, surface ice temperature, and heat absorption. Alternatively, fields from a 3-year model climatology can be used.

NRL tested PIPS for operational use by comparing PIPS-derived ice motion with that from buoy data, and that from JIC's existing free-drift model. Ice-edge location derived by PIPS was compared with that from the JIC analysis. In 1987, PIPS was declared operational. The model is run daily at FNOC, where the computational requirements and need for access to forcing data can be met. Each run produces a 120-h forecast, with model results output at every 6-h timestep. Graphic products, such as ice drift, thickness, and concentration, are sent to JIC over the NEDS.

Satellite data can be used to improve model forecasts by providing fields for model initialization, updates, or verification, or by providing parameters needed in forcing terms. Of the fields that PIPS uses for initialization, three can potentially be provided by remote sensing data: concentration, ice drift, and surface ice temperature. In addition, ice type derived from imagery may be adequate for creating an ice thickness field, or at least for providing the coverage of thin ice and open water. Satellite data are currently used by PIPS in an indirect manner, when the ice concentration field is updated once per week with a digitized version of the JIC ice analysis. The accuracy and timeliness of this analysis can drastically affect PIPS forecasts. Because the JIC analysis depends primarily on AVHRR, one way to improve the PIPS forecast is to improve the JIC analysis by facilitating the use of microwave sensors at JIC, as discussed in the sections on SSM/I and SAR.

The timeliness with which the ice concentration field is updated could be improved by using concentration derived directly from SSM/I. This is valid only if the SSM/I concentrations are an improvement over concentration derived from other sources. Rothrock and Thomas (1988) point out an uncertainty of several degrees in the brightness temperature of the ice surface. They account for this uncertainty by using a physical model of ice-type concentration in conjunction with SMMR data. The model prevents changes in passive microwave brightness temperature from being interpreted as unrealistic changes in ice-type concentration (see SSM/I section). It may be possible to use a similar bootstrapping technique for assimilating SSM/I into the PIPS model.

SAR can give accurate estimates of ice drift and of the amount of thin ice in an area (an important model parameter), but the scale of SAR coverage is not well matched to the PIPS grid resolution of 127 km. For instance, a single ERS-1 SAR image would fit within a grid cell. However, regional models, such as PIPS models for the Greenland and Barents Seas, have smaller

grid cells, making them more amenable to initialization or updating with SAR imagery. The PIPOR proposal (PIPOR Research Plan 1989) plans to demonstrate the inclusion of SAR data in regional model initialization fields and the use of SAR for model verification. (In addition, ice concentration from SSM/I will be compared with that from SAR).

AVHRR could conceivably be used to provide a surface temperature field (see AVHRR section) and an ice drift field. As with fields provided by SAR, spatial coverage is not complete, and schemes must be devised for assimilating data into the model directly or for optimally interpolating to arrive at the best possible composite field from many sources. Those hoping to derive ice characteristics from data fusion are faced with the same challenge.

In addition to providing fields for updating a model, remote sensing may be used to obtain some of the forcing parameters. McNutt et al. (1988) look at information from remote sensing in comparison with that from point sources and physical models (including the products of remote sensing algorithms and climatologies) in terms of its ability to supply parameters needed by most operational forecasting models (Fig. 8). With the exception of wind and air temperature, all parameters can be arrived at through satellite data (although some require a time history, and some techniques are still experimental). While one may argue about parameters chosen for Fig. 8 and about the ability of a given sensor to measure them with the accuracy and on a scale required by models, the figure emphasizes that satellite sensors compare well with other means of providing information to models.

Remote sensing may also be used to refine estimates of forcing parameters. For instance, Burns and Wegener (1988) suggested that ice surface roughness derived from SAR image backscatter can be used to estimate spatial variation in the drag coefficient for a better estimate of wind stress. Albedo, cloud cover, and surface temperature from AVHRR can be used to improve heat flux estimates.

VII. RECOMMENDATIONS—MODEL INPUT FROM REMOTE SENSING

A workshop for NRL participants to establish priorities and a timetable for research leading to the integration of polar satellite data and numerical models would benefit both modelers and the Remote Sensing Applications Branch.

VIII. CONCLUSIONS

It is appropriate for the major emphasis in automated analysis ice work to be placed on automated interpretation of SAR imagery over the next several years. A SAR image can produce more information useful to operational ice analysis than can an image from another sensor covering the same area, and future SARs promise near-synoptic coverage. The challenge of extracting that information can be met through automated analysis techniques.

SSM/I imagery cannot be neglected, yet because its resolution is too low to distinguish most ice features and a simple tiepoint algorithm can extract the image's information content, the imagery by itself does not lend itself to new automated analysis techniques. SSM/I data can be merged with other data, and work can be done to improve the accuracy of SSM/I algorithms.

AVHRR will continue to be the primary data source at JIC. Canned enhancements and a cloud-masking routine can be developed for use on DIFAS, but there is no pressing need for this.

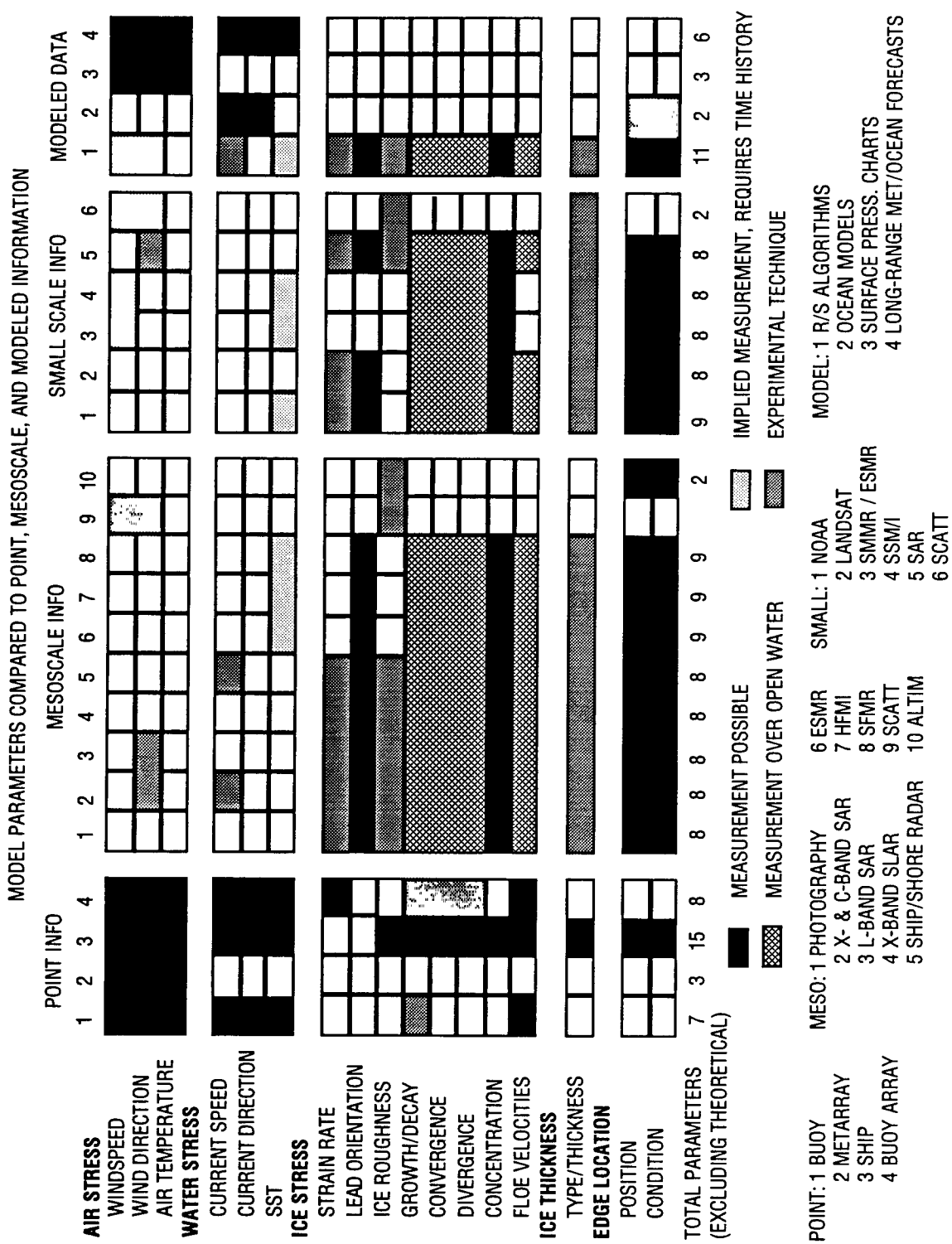


Fig. 8 — Parameters needed by most operational forecasting models and data sources for those parameters (from McNutt et al. 1988)

Altimetry will remain important for mapping the ice edge. Work with altimetry over sea ice should include a study to determine the best global ice index and to determine how an ice index responds to variable MIZ conditions.

Accomplishing four milestones could be pivotal in ensuring that rapid progress toward the goal of a comprehensive ice analysis system is made over the next 5 years. Recommendations put forth in previous sections contribute to or rely upon these milestones, and can be carried out as resources and interest warrant. Figure 9 shows a timeline for work on the following milestones:

- Develop methods for extracting ice parameters from merged data sets consisting of, for instance, AVHRR and SSM/I data, and including other data, such as altimetry, meteorological fields, and SAR imagery when appropriate.

— In addition to work on classifying merged data on a pixel-by-pixel basis, this milestone is meant to encourage work, such as using the altimeter in conjunction with AVHRR and SSM/I for ice edge conditions, using SAR to improve SSM/I algorithm results, or using surface temperatures derived from meteorological fields or AVHRR to put confidence limits on ice type from SSM/I or SAR. These applications, which make use of merged data, can eventually be pieces of a more comprehensive ice analysis system. Several coincident data sets should emerge as research on algorithms is carried out, since improved algorithms will usually require multiple data sources for input or validation.

- Create a prototype SAR automated analysis system for Beaufort Sea ice analysis.

— A prototype system can be created during the ERS-1 SAR lifetime. It can be driven by simple rules applied to image features for which algorithms are already developed (although not validated). As a second step, the system can be made to search a data base for near-coincident data from other sources, register it to the SAR imagery, and thereby have more information on which to base decisions. Although it is unlikely that this step will prove truly useful with the prototype

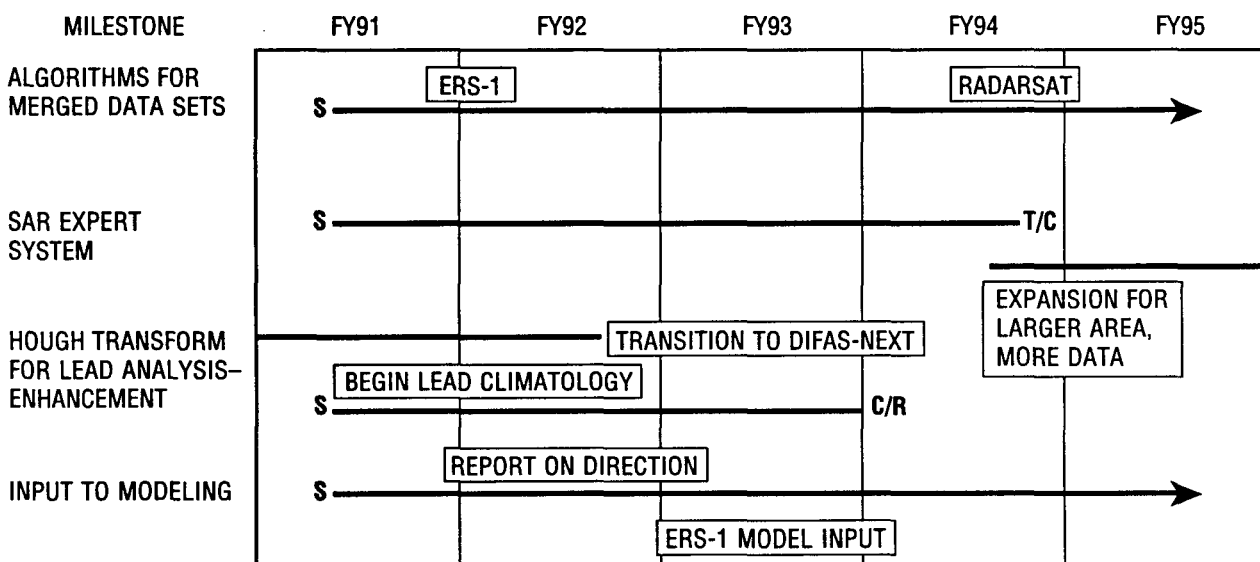


Fig. 9 — Ice analysis milestone timetable

system, since the resolution of SAR exceeds that of other sensors and location accuracy is a problem, it illustrates a method of linking data sets for such applications as those in the first milestone. Experience gained in building a prototype system for the Beaufort Sea can be applied to a more evolved system for Radarsat and EOS imagery.

- Complete development of the Hough transform method for lead statistics. Begin compiling a lead climatology using the Hough transform method and AVHRR imagery processed for the Arctic Leads ARI.

— Development of the Hough transform method is nearly complete. Work remains to be done on automatically creating a binary lead image. A rule-based system for defining leads and extracting statistics based on those definitions should be incorporated. The demonstrated use of a high-level automated interpretation technique for creating an operationally important climatology will boost confidence in the usefulness of automated interpretation techniques for ice analysis. For this reason, the milestone should be completed as soon as is practical.

- Develop methods of assimilating satellite-derived ice information into ice prediction models.

— This work has begun under the 6.3 SSM/I Ocean Application program, but many issues need to be addressed before the application of other satellite data to ice modeling can go forward.

The Remote Sensing Applications Branch can contribute several strengths for solving the problems of the automated analysis of sea ice data: wide-ranging expertise in automated analysis and artificial intelligence techniques, experience in bringing techniques together in an operational system (through the Geosat Ocean Applications Program), a continually improving understanding of operational needs through ties with JIC, and nearly unlimited access to satellite data from operationally important sensors.

IX. ACKNOWLEDGMENTS

This report was initiated and guided by Dr. Ron Holyer, manager of the 6.2 Automated Data Analysis Task of the Data Assimilation and Analysis Project. The report benefited by contributions from Dr. Duane Eppler, formerly of the Naval Oceanographic and Atmospheric Research Laboratory's Polar Oceanography Branch, and Mr. Jeffrey Hawkins, formerly of NRL's Remote Sensing Applications Branch. The work was supported by the Office of Naval Research under Program Element 0602435N. CDR Lee Bounds was the program manager.

X. REFERENCES

- Askne, J. and R. Johansson, "Ice Ridge Observations by Means of SAR," Proceedings, International Geoscience and Remote Sensing Symposium, Edinburgh, Scotland, September 13–16, 1988.
- Banfield, J. D. and A. E. Raftery, "Ice Floe Identification in Satellite Images using Mathematical Morphology and Clustering Around Principal Curves," Department of Mathematical Sciences, Montana State University, Bozeman, MT, 1989, 32 pp.
- Burns, B. A. and A. Wegener, "SAR Image Statistics Related to Atmospheric Drag Over Sea Ice," Proceedings, International Geoscience and Remote Sensing Symposium, Edinburgh, Scotland, September 13–16, 1988.

- Burns, B. A., R. R. Jentz, C. G. Caruthers, J. D. Lyden, and P. L. Jackson, "Computer Assisted Techniques for Geophysical Analysis of SAR Sea Ice Imagery," Proceedings, International Geoscience and Remote Sensing Symposium, Ann Arbor, MI, October 21–25, 1985.
- Carsey, F. D. and H. J. Zwally, "Remote Sensing as a Research Tool," in *The Geophysics of Sea Ice*, (New York and London, Plenum Press, 1986), 1196 pp. (NATO ASI series. Seris B, Physics; vol. 146).
- Cavalieri, D. J., J. P. Crawford, M. Drinkwater, D. T. Eppler, L. D. Farmer, R. R. Jentz, and C. C. Wackerman, "Aircraft Active and Passive Microwave Validation of Sea Ice Concentration from the DMSP SSM/I," *Journal of Geophysical Research*, in press.
- Chase, J. R. and R. J. Holyer, "Estimation of Sea-ice Type and Concentration by Linear Unmixing of GEOSAT Altimeter Waveforms," Proceedings, International Geoscience and Remote Sensing Symposium, Edinburgh, Scotland, September 13–16, 1988.
- Condal A. R. and H. V. Le, "Automated Computer Monitoring Sea-Ice Temperature by Use of NOAA Satellite Data," Proceedings, Eighth Canadian Symposium on Remote Sensing, 1984.
- Condal, A. R., B. Wannamaker, and H. V. Le, "The Ice Status System and Application of NOAA Satellite Data to Sea Ice Monitoring," Proceedings, Ninth Canadian Symposium on Remote Sensing, 1985.
- Daida, J., R. Samadani, and J. Vesecky, "Object-Oriented Feature-Tracking Algorithms for SAR Images of the Marginal Ice Zone," *IEEE Transactions on Geoscience and Remote Sensing* 28(4), 573–589 (1990).
- Ebert, E. E., "Satellite Observation of High Latitude Surface and Cloud Types Using Pattern Recognition," Proceedings, Second Conference on Polar Meteorology and Oceanography, Madison, WI, March 29–31, 1988.
- Eppler, D. T., L. D. Farmer, and D. J. Cavalieri, "Regional Variation in Multiyear Sea Ice Brightness Temperature," presented at North American Sea Ice Workshop, Amherst, MA, June 26–28, 1989.
- Fetterer, F. and R. J. Holyer, "A Hough Transform Technique for Extracting Lead Features from Sea Ice Imagery," Proceedings, International Geoscience and Remote Sensing Symposium, Vancouver, Canada, July 10–14, 1989.
- Fetterer, F., D. Johnson, J. Hawkins, and S. Laxon, "Investigations of Sea Ice Using Coincident GEOSAT Altimetry and Synthetic Aperture Radar During MIZEX-87," Proceedings, International Geoscience and Remote Sensing Symposium, Edinburgh, Scotland, September 13–16, 1988.
- Fetterer, F., A. E. Pressman, and R. Crout, "Sea Ice Lead Statistics from Satellite Imagery of the Lincoln Sea During the ICESHELF Acoustic Exercise, Spring 1990," Naval Research Laboratory, Stennis Space Center, MS, NOARL Technical Note 50, 1990.
- Fu, L. and B. Holt, "Seasat Views Oceans and Sea Ice with Synthetic Aperture Radar," Jet Propulsion Laboratory, California Institute of Technology, Pasadena, CA, JPL Publication 81–120, 1982.

- Garcia, F. G., "Sea Ice Classification Using Synthetic Aperture Radar," Master thesis, Naval Postgraduate School, Monterey, CA (NPS-68-90-004), 1990.
- Gerson, D. J. and A. Rosenfeld, "Automatic Sea Ice Detection in Satellite Pictures, *Remote Sensing of Environment* 4, 187–198 (1975).
- Hawkins, J., "Altimeter Sea Ice Workshop," Naval Research Laboratory, Stennis Space Center, MS, NOARL Special Project 059:321:90, 1990.
- Hirose, T., Patterson, S., and L. McNutt, "A Study of Textural and Tonal Information for Classifying Sea Ice Imagery from SAR Imagery," presented at the North American Sea Ice Workshop, Amherst, MA, June 26–28, 1989.
- Holback-Hanssen, E., Tjelmeland, H., Johannessen, O. M., Olaussen, T., and Karpue, R., "Speckle Reduction and Maximum Likelihood Classification of SAR Images from Service Recorded During MIZEX 8F," Proceedings of the International Geoscience and Remote Sensing Symposium, July 10–14, 1989, Vancouver, Canada, 1989, pp. F55–F58.
- Holmes, Q. A., D. R. Nuesch, and R. A. Shuchman, "Textural Analysis and Real-Time Classification of Sea-Ice Types Using Digital SAR Data," *IEEE Transactions on Geoscience and Remote Sensing* 22(2), 113–120 (1984).
- Holt, B., R. Kwok, and E. Rignot, "Ice Classification Algorithm Development and Verification for the Alaska SAR Facility Using Aircraft Imagery," Proceedings, International Geoscience and Remote Sensing Symposium, Vancouver, Canada, July 10–14, 1989.
- Holyer, R. J., "A Global Approach to Image Texture Analysis," Ph.D. dissertation, Department of Geological Sciences, University of South Carolina, 1989.
- Hufford, G. L., "Sea Ice Detection Using Enhanced Infrared Satellite Data, *Mariners Weather Log* 25(1), 1:6 (1981).
- Joint Oceanographic Institutions, Inc., "Operational Products from Ocean Satellites: Issues of Algorithm Development and Data Assimilation for NOAA," Volume 1. L. Lynch, ed. Study supported by JPL Contract #957522, 1987.
- Key, J., "Cloud Cover Analysis with Arctic Advanced Very High Resolution Radiometer Data 2," classification with spectral and textural measures, *Journal of Geophysical Research* 95(D6), 7661–7675 (1990).
- Key, J. and R. G. Barry, "Cloud Cover Analysis with Arctic AVHRR Data 1," cloud detection, *Journal of Geophysical Research* 94(D15), 18521–18535 (1989).
- Key, J., J. Maslanik, and A. J. Schweiger, "Classification of Merged AVHRR and SMMR Arctic Data with Neural Networks," *Photogrammetric Engineering and Remote Sensing* 55(9), 1331–1338 (1989).
- Key, J., A. J. Schweiger, and J. A. Maslanik, "Mapping Sea Ice Leads with a Coupled Numeric/Symbolic System," presented at the American Society of Photogrammetry and Remote Sensing Conference, Boulder, CO, March 1990.

- Kwok, R., J. Curlander, R. McConnell, and S. Pang, "An Ice-Motion Tracking System at the Alaska SAR Facility, *IEEE Journal of Oceanic Engineering* 15(1), 44–54 (1990).
- Laxon, S., "Sea Ice Operational Products from Space Borne Radar Altimeters," presented at 15th Annual Conference of the Remote Sensing Society, University of Bristol, UK, September 13–15, 1989a.
- Laxon, Seymour William Clarke, "Satellite Radar Altimetry Over Sea Ice," Ph.D. thesis, Mullard Space Science Laboratory, University College, London, UK, 1989b.
- Lee, M., "Sea-Ice Analysis Software—ICEMAN," Proceedings, International Geoscience and Remote Sensing Symposium, Edinburgh, Scotland, September 13–16, 1988.
- Livingstone, C. E., K. P. Singh, and A. L. Gray, "Seasonal and Regional Variations of Active/Passive Microwave Signatures of Sea Ice, *IEEE Transactions on Geoscience and Remote Sensing* 25(2), 159–172 (1987).
- Lyden, J., B. Burns, and A. Maffett, "Characterization of Sea Ice Types Using Synthetic Aperture Radar," *IEEE Transactions on Geoscience and Remote Sensing* 22(5), 431–439 (1984).
- Maslanik, J. A., J. R. Key, and R. G. Barry, "Merging AVHRR and SMMR Data for Remote Sensing of Ice and Cloud in Polar Regions, *International Journal of Remote Sensing* 10(10), 1691–1696 (1989).
- McAvoy, J. G. and E. M. Krakowski, "A Knowledge Based System for the Interpretation of SAR Images of Sea Ice," Proceedings, International Geoscience and Remote Sensing Symposium, Vancouver, Canada, July 10–14, 1989.
- McIntyre, N., "Radar Altimetry Over Sea Ice," Proceedings of the International Conference of the Remote Sensing Society and the Center for Earth Resources Management, London, UK, September, 1985.
- McNutt, L., T. Mullane, and T. Hirose, "Toward the Automated Use of Remote Sensing Data in Operational Ice Forecasting," Proceedings, International Geoscience and Remote Sensing Symposium, Edinburgh, Scotland, September 13–16, 1988.
- Preller, R. H. and P. G. Posey, "The Polar Ice Prediction System—A Sea Ice Forecasting System," Naval Research Laboratory, Stennis Space Center, MS, NOARL Report 212, 1989.
- "Programme for International Polar Oceans Research (PIPOR) ERS-1 Research Plan," L. McNutt/Th. Viehoff, eds., PI Summary Document, Ottawa/Bremerhaven, December 1989.
- Ramsey, B. R. and M. A. Zieger, "Enhancement of NOAA AVHRR Digital Data for Sea Ice Analysis in an Operational Environment," presented at Bedford Institute of Oceanography Workshop on Sea Ice, Bedford, Canada, Jan. 1986.
- Robin, G., D. J. Drewry, and V. A. Squire, "Satellite Observations of Polar Ice Fields," *Philosophical Transactions of the Royal Society of London* A309:447–461 (1983).

- Rothrock, D. A. and D. R. Thomas, "Estimating Sea Ice Concentration from Satellite Passive Microwave Data and a Physical Model," Proceedings, International Geoscience and Remote Sensing Symposium, Edinburgh, Scotland, September 13–16, 1988.
- Schweiger, A. J. and K. Steffen, "Comparison of Sea Ice Parameters Retrieved from Passive Microwave (SSM/I), Landsat MSS, and AVHRR Imagery, Proceedings, International Geoscience and Remote Sensing Symposium, Vancouver, Canada, July 10–14, 1989.
- Shirliffe, G. M., "Expert System Design for Radar Reconnaissance of Sea Ice," Proceedings, International Geoscience and Remote Sensing Symposium, Vancouver, Canada, July 10–14, 1989.
- Shokr, M. E., "On Sea-Ice Texture Characterization from SAR Images," *IEEE Transactions on Geoscience and Remote Sensing* **28**(4), 737–740 (1990).
- Skriver, H., P. Gudmandsen, and L. Ulander, "Active Microwave Observations of Sea Ice and Iceberg," Proceedings of the SAR Applications Workshop, Frascati, Italy, Sept. 1986.
- Schweiger, A. and K. Steffen, "Sensitivity of Passive Microwave Sea Ice Concentration Algorithms to the Selection of Locally and Seasonally Adjusted Tiepoints," Proceedings, International Geoscience and Remote Sensing Symposium, Vancouver, Canada, July 10–14, 1989.
- Ulander, L., "Observations of Ice Types in Satellite Altimeter Data," Proceedings, International Geoscience and Remote Sensing Symposium, Edinburgh, Scotland, September 13–16, 1988.
- Ulander, L., "Interpretation of Seasat Radar-Altitude Data Over Sea Ice Using Near-Simultaneous SAR Imagery," *International Journal of Remote Sensing* **8**(11), 1679–1686 (1987).
- Vesecky, J., M. Smith, and R. Samadani, "Extraction of Lead and Ridge Characteristics from SAR Images of Sea Ice," *IEEE Transactions on Geoscience and Remote Sensing* **28**(4), 573–589 (1990).
- Wackerman, C., R. Jentz, and A. Shuchman, "Sea Ice Type Classification of SAR Imagery," Proceedings, International Geoscience and Remote Sensing Symposium, Edinburgh, Scotland, September 13–16, 1988.
- Wadhams, P., A. S. McLaren, and R. Weintraub, "Ice Thickness Distribution in Davis Strait in February from Submarine Sonar Profiles," *Journal of Geophysical Research* **90**(C1), 1069–1077 (1985).